Factors governing the magnitude of Δ_{oct}

1- Oxidation state of the metal ion

For a given ligand and a given metal, Δ_{oct} increases with increasing oxidation state(see table(9),the value of Δ_{oct} for Fe(3+) complex is larger than of Fe(2+) complex. This effect is probably due to the fact that the central ion with higher oxidation state will polarize the ligands more effectively and thus the ligands would approach such a cation more closely than they can do the cation of lower oxidation state, resulting in larger splitting.

Table(9) shows values of Δ_{oct} for some d-block metal

Complex	Δ / cm^{-1}	Complex	Δ / cm^{-1}
$[TiF_6]^{3-}$	17 000	$[Fe(ox)_3]^{3-}$	14 100
$[Ti(OH_2)_6]^{3+}$	20 300	$[Fe(CN)_6]^{3-}$	35 000
$[V(OH_2)_6]^{3+}$	17 850	$[Fe(CN)_6]^{4-}$	33 800
$[V(OH_2)_6]^{2+}$	12 400	$[CoF_6]^{3-}$	13 100
$[CrF_6]^{3-}$	15 000	$[Co(NH_3)_6]^{3+}$	22 900
$[Cr(OH_2)_6]^{3+}$	17 400	$[Co(NH_3)_6]^{2+}$	10 200
$[Cr(OH_2)_6]^{2+}$	14 100	$[Co(en)_3]^{3+}$	24 000
$[Cr(NH_3)_6]^{3+}$	21 600	$[Co(OH_2)_6]^{3+}$	18 200
$[Cr(CN)_6]^{3-}$	26 600	$[Co(OH_2)_6]^{2+}$	9 300
$[MnF_6]^{2-}$	21 800	$[Ni(OH_2)_6]^{2+}$	8 500
$[Fe(OH_2)_6]^{3+}$	13 700	$[Ni(NH_3)_6]^{2+}$	10 800
$[Fe(OH_2)_6]^{2+}$	9 400	$[Ni(en)_3]^{2+}$	11 500

2- Nature of metal ion

Δ_{oct} varies irregularly across the first row of the d-block, e.g. over the range 8000 to 14 000 cm^{-1} for the $[M(OH_2)_6]^{2+}$ ions(see table(9)).

Trends in values of Δ_{oct} lead to the conclusion that metal ions can be placed in a spectrochemical series which is independent of the ligands:

Mn(II)<Ni(II)<Co(II)<Fe(III)<Cr(III)<Co(III)<Ru(III)
<Mo(III)<Rh(III)<Pd(II)< Ir(III)<Pt(IV)

increasing of Δ_{oct} value

3- Quantum number (n) of the d-orbital of the central metal ion.

For analogous complexes exist for a series of M^{n+} metals ions (constant n) in a triad, Δ_{oct} increases significantly down the triad, Δ_{oct} increase 50% from 3d to 4d and 25% from 4d to 5d.

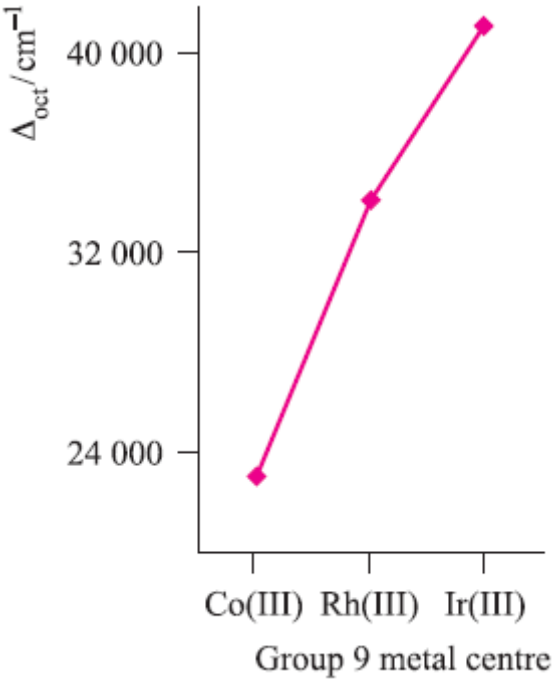

Fig. Shows the trend in values of Δ_{oct} for the complexes $[M(NH_3)_6]^{3+}$ where M = Co, Rh, Ir.

i.e. Δ_{oct} values increase as we go down the periodic table ***3d <<4d<5d.*** This might be compatible with the electrostatic model in that the radial extensions of *4d* and 5*d* orbitals are greater than that of *3d*.

4- Nature of the ligands

The common ligands can be ordered on the basis of the effect that they have on the crystal field splitting. This ordered listing is called the ***spectrochemical series***. Among the common ligands, the splitting is largest with carbonyl and cyanide and smallest with iodide .The complexes of Cr(III) listed in Table (9)

illustrate the effects of different ligand field strengths for a given M^{n+} ion, for octahedral complexes,; the NCS^- ion may coordinate through the N^- or S^- donor (distinguished in dark below) and accordingly, it has two positions in the series:

CO, CN^- > phen > NO_2^- > en > NH_3 > **N**CS^- > H_2O~$OX^=$ > F^- > RCO_2^- > OH^- > $C1^-$ >NC**S**$^-$> Br^- > I^-

Crystal field stabilization energy(CFSE): high- and low-spin octahedral complexes

We now consider the effects of different numbers of electrons occupying the d orbitals in an octahedral crystal field. For a $\mathbf{d^1}$ system, the ground state corresponds to the configuration t_{2g}^1. With respect to the barycentre, there is a stabilization energy of $-0.4\Delta_{oct}$; this is the so-called crystal field stabilization energy, CFSE. For a $\mathbf{d^2}$ ion, the ground state configuration is t_{2g}^2 and the CFSE = $-0.8\Delta_{oct}$. A $\mathbf{d^3}$ ion (t_{2g}^3) has a CFSE = $-1.2\Delta_{oct}$.

For electrons in t_{2g} and eg ;

$$\mathbf{CFSE = n \times (-0.4\Delta_{oct}) + n \times (+0.6\Delta_{oct})} \text{ (n=number of electrons)}$$

For a ground state $\mathbf{d^4}$ ion, two arrangements are available: the four electrons may occupy the t_{2g} set with the configuration t_{2g}^4 (**a**), or may singly occupy four d orbitals, $t_{2g}^3e_g^1$ (**b**).

a **b**

Configuration (**a**) corresponds to a low-spin arrangement, and (**b**) to a high-spin case. The preferred configuration is that with the lower energy and depends on

whether it is energetically preferable to pair the fourth electron or promote it to the e_g level. Two terms contribute to the electron-pairing energy, P, which is the energy required to transform two electrons with parallel spin in different degenerate orbitals into spin-paired electrons in the same orbital:

a- The loss in the exchange energy which occurs upon pairing the electrons.

b- The coulombic repulsion between the spin-paired electrons.

For a given $\mathbf{d^n}$ configuration, the CFSE is the difference in energy between the **d** electrons in an octahedral crystal field and the **d** electrons in a spherical crystal field. To exemplify this, consider a $\mathbf{d^4}$ configuration. In a spherical crystal field, the d orbitals are degenerate and each of four electrons is singly occupied. In an octahedral crystal field, equation below shows how the CFSE is determined for a high-spin $\mathbf{d^4}$ configuration.

$$\mathbf{CFSE = 3 \times (-0.4\Delta_{oct}) + 1 \times (+0.6\Delta_{oct}) = -0.6\Delta_{oct}}$$

For a low-spin $\mathbf{d^4}$ configuration, the CFSE consists of two terms: the four electrons in the t_{2g} orbitals give rise to a $-1.6\Delta_{oct}$ term, and a pairing energy, **P**, must be included to account for the spin-pairing of two electrons. Now consider a $\mathbf{d^6}$ ion. In a spherical crystal field, one **d** orbital contains spin-paired electrons, and each of four orbitals is singly occupied. On going to the high-spin $\mathbf{d^6}$ configuration in the octahedral field ($t_{2g}^4 e_g^2$), no change occurs to the number of spin-paired electrons and the CFSE is given by equation below.

$$\mathbf{CFSE = 4 \times (-0.4\Delta_{oct}) + 2 \times (+0.6\Delta_{oct}) = -0.4\Delta_{oct}}$$

For a low-spin d^6 configuration ($t_{2g}^6 e_g^0$) the six electrons in the t_{2g} orbitals give rise to a $-2.4\Delta_{oct}$ term. Added to this is a pairing energy term of **2P** which accounts for the

spin pairing associated with the two pairs of electrons in excess of the one in the high-spin configuration. Table (10) lists values of the CFSE for all $\mathbf{d^n}$ configurations in an octahedral crystal field. Inequalities (**a**) and (**b**) show the requirements for high- or low-spin configurations. Inequality (**a**) holds when the crystal field is weak, whereas expression (**b**) is true for a strong crystal field.

For high-spin: $P > \Delta_{oct}$ (a)

For low-spin: $P < \Delta_{oct}$ (b)

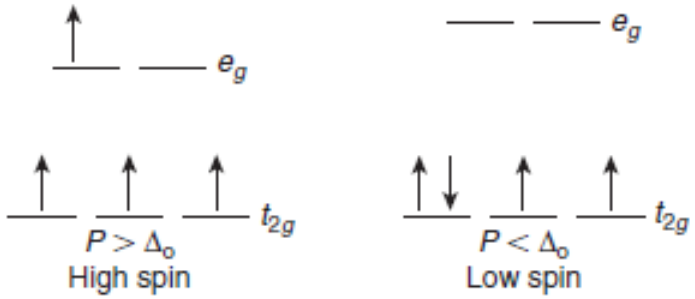

Figure below summarizes the preferences for low- and high-spin d^5 octahedral complexes.

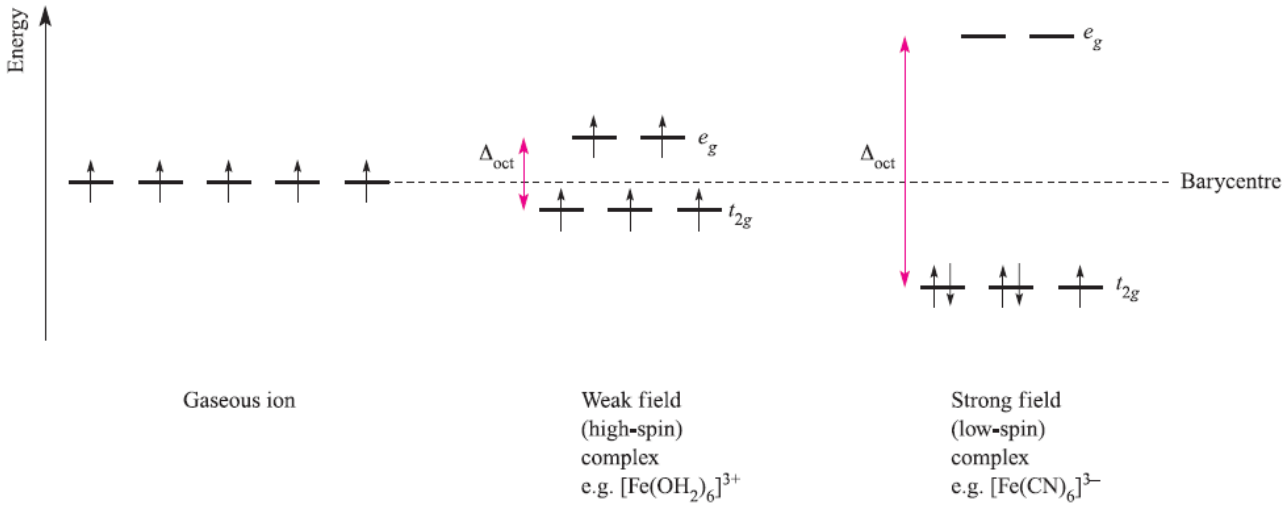

Fig, shows; the occupation of the 3d orbitals in weak and strong field Fe^{3+} (d^5) complexes.

We can now relate types of ligand with a preference for high- or low-spin complexes. Strong field ligands such as $[CN]^-$ favour the formation of low-spin complexes, while weak field ligands such as halides tend to favour high-spin complexes. However, we cannot predict whether high- or low-spin complexes will be formed unless we have accurate values of Δ_{oct} and P. On the other hand, with some experimental knowledge in hand, we can make some comparative predictions: if we know from magnetic data that $[Co(OH_2)_6]^{3+}$ is low-spin, then from the spectrochemical series we can say that $[Co\ (ox)_3]^{3-}$ and $[Co(CN)_6]^{3-}$ will be low-spin. The only common high-spin cobalt(III) complex is $[CoF_6]^{3-}$.

Table (10); Octahedral crystal field stabilization energies (CFSE) for d^n configurations; pairing energy, P, terms are included where appropriate. High- and low-spin octahedral complexes are shown only where the distinction is appropriate.

d^n	High-spin = weak field		Low-spin = strong field	
	Electronic configuration	CFSE	Electronic configuration	CFSE
d^1	$t_{2g}^1 e_g^0$	$-0.4\Delta_{oct}$		
d^2	$t_{2g}^2 e_g^0$	$-0.8\Delta_{oct}$		
d^3	$t_{2g}^3 e_g^0$	$-1.2\Delta_{oct}$		
d^4	$t_{2g}^3 e_g^1$	$-0.6\Delta_{oct}$	$t_{2g}^4 e_g^0$	$-1.6\Delta_{oct} + P$
d^5	$t_{2g}^3 e_g^2$	0	$t_{2g}^5 e_g^0$	$-2.0\Delta_{oct} + 2P$
d^6	$t_{2g}^4 e_g^2$	$-0.4\Delta_{oct}$	$t_{2g}^6 e_g^0$	$-2.4\Delta_{oct} + 2P$
d^7	$t_{2g}^5 e_g^2$	$-0.8\Delta_{oct}$	$t_{2g}^6 e_g^1$	$-1.8\Delta_{oct} + P$
d^8	$t_{2g}^6 e_g^2$	$-1.2\Delta_{oct}$		
d^9	$t_{2g}^6 e_g^3$	$-0.6\Delta_{oct}$		
d^{10}	$t_{2g}^6 e_g^4$	0		

The Jahn-Teller Effect

The Jahn-Teller theorem' states that there cannot be unequal occupation of orbitals with identical energies. To avoid such unequal occupation, the molecule distorts so that these orbitals are no longer degenerate. For example, octahedral Cu(II), a d^9 ion, would have three electrons in the two e_g levels without the Jahn-Teller effect, as in the center of Figure (below). The Jahn-Teller effect requires that the shape of the complex change slightly, resulting in a change in the energies of the

orbitals. The resulting distortion is most often an elongation along one axis, but compression along one axis is also possible. **In octahedral complexes**, where the *eg* orbitals are directed toward the ligands, distortion of the complex has a larger effect on these energy levels and a smaller effect when the t_{2g} orbitals are involved.

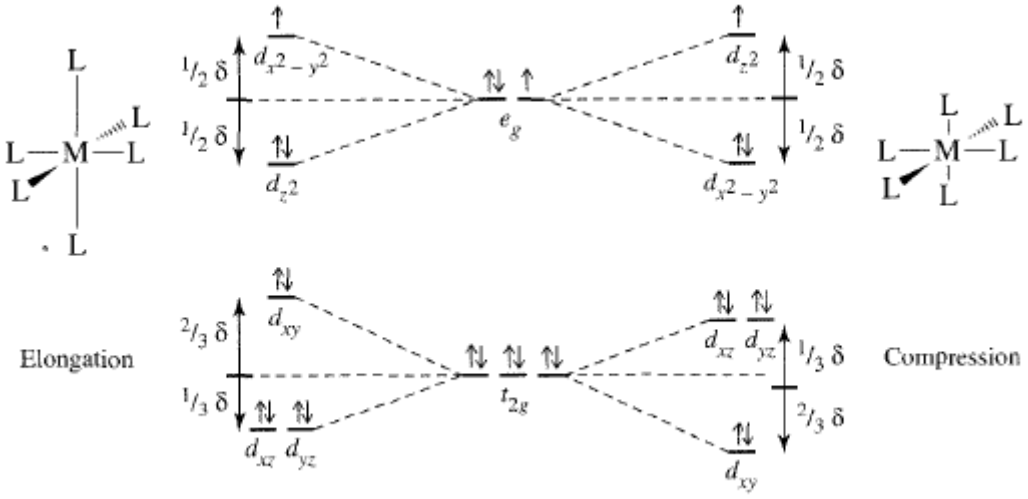

Figure: shows Jahn-Teller Effect on a d^9 Complex. Elongation along the *z* axis is coupled to a slight decrease in bond length for the other four bonding directions. Similar changes in energy result when the axial ligands have shorter bond distances. The resulting splits are larger for the e_g orbitals than for the t_{2g}.

The effect of both elongation **(Z-out)** and compression **(Z-in)** on **d** orbital energies is shown in Figure (above), and the expected Jahn- Teller effects are summarized in the following table:

Number of electrons	1	2	3	4	5	6	7	8	9	10
High-spin Jahn-Teller	w	w		s		w	w		s	
Low-spin Jahn-Teller	w	w		w	w		s		s	

w = weak Jahn-Teller effect expected (t_{2g} orbitals unevenly occupied); s = strong Jahn-Teller effect expected (e_g orbitals unevenly occupied); No entry = no Jahn-Teller effect expected.

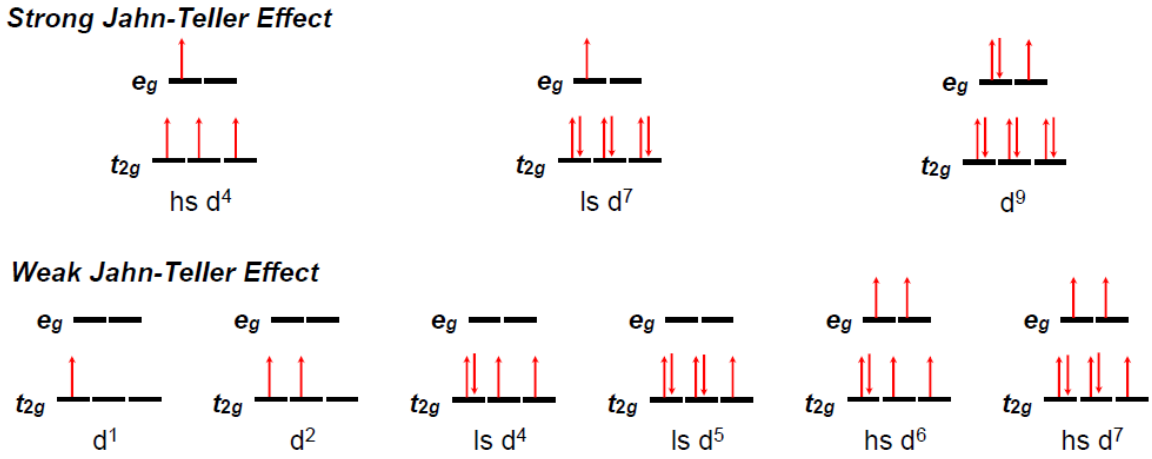

Z-out distortion: In this case, the energies of d-orbitals with z factor (i.e., d_z2, d_{xz}, d_{yz}) are *lowered* since the bonds along the z-axis are elongated. This is the most preferred distortion and occurs in most of the cases, especially when the degeneracy occurs in e_g level.

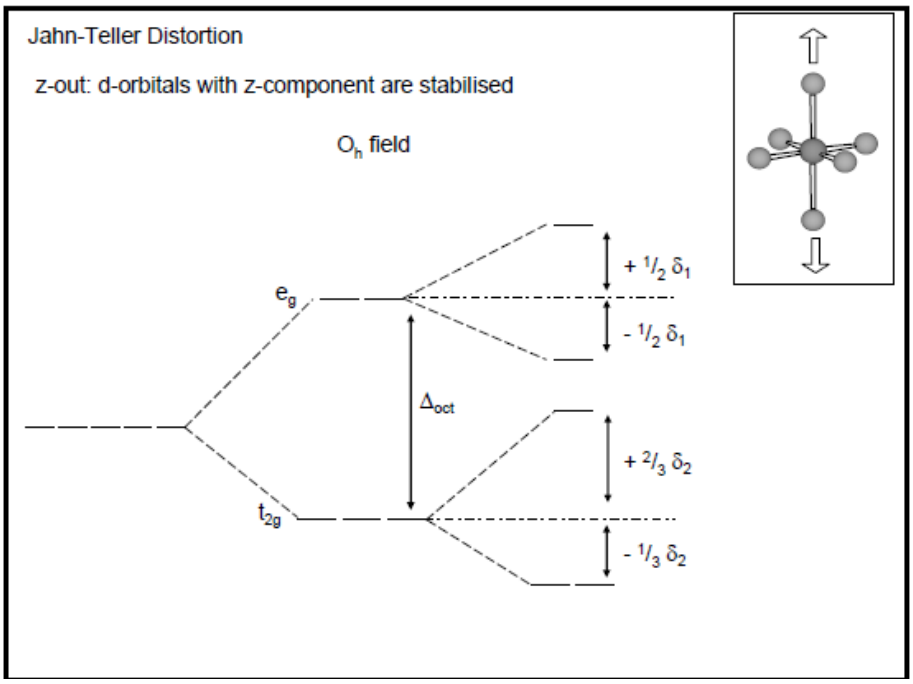

E.g. Usually the octahedral d^2, d^4 high spin, d^7 low spin, d^8 low spin & d^9 configurations show the z-out distortion.

Theoretically it is not possible to predict the type of distortion occurs when the degeneracy occurs in e_g level. However it is observed that z-out distortion is more preferred.

Z-in distortion: In this case the energies of orbitals with z factor are *increased* since the bonds along the z-axis are shortened. This type of distortion is observed in case of octahedral d^1 configuration. The only electron will now occupy the d_{xy} orbital with lower energy.

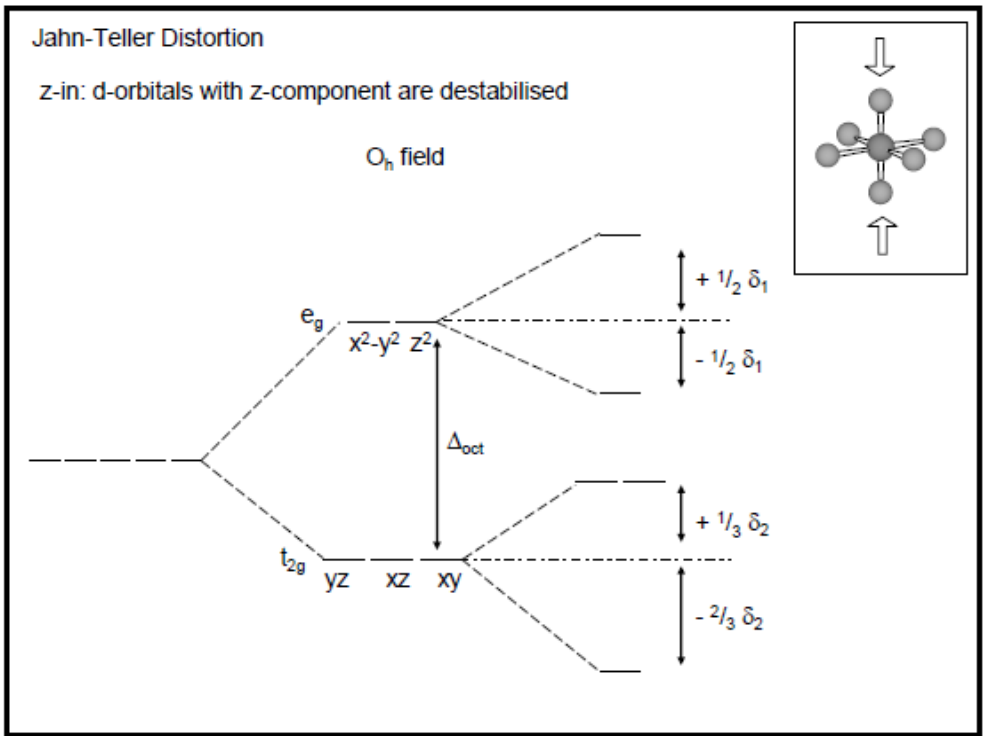

E.g. The octahedral d^1 configurations like Ti(III) in $[Ti(H_2O)_6]^{3+}$ can show z-in distortion (theoretically?). In this case, the z-out distortion do not remove the degeneracy since even after distortion there are still two degenerate orbitals i.e., d_{xz} and d_{yz} available for the electron to occupy.

.

Elongation (Z-out) plays a part in the change in equilibrium constants for complex formation. For example, $[Cu(NH_3)_4(H_2O)_2]^{2+}$ is readily formed in aqueous solution as a distorted octahedron with two water molecules at larger distances than the ammonias, but liquid ammonia is required for formation of the hexammine

complex$[Cu(NH_3)_6]^{2+}$. The formation constants for these reactions show the difficulty of putting the fifth and sixth ammonias on the metal. Which factor is the cause and which the result is uncertain, but the bond distances for the two axial positions are longer than those of the four equatorial positions, and the equilibrium constants are much smaller.

$$[Cu(H_2O)_6]^{2+} + NH_3 \rightleftharpoons [Cu(NH_3)(H_2O)_5]^{2+} + H_2O \qquad K_1 = 2 \times 10^4$$
$$[Cu(NH_3)(H_2O)_5]^{2+} + NH_3 \rightleftharpoons [Cu(NH_3)_2(H_2O)_4]^{2+} + H_2O \qquad K_2 = 4 \times 10^3$$
$$[Cu(NH_3)_2(H_2O)_4]^{2+} + NH_3 \rightleftharpoons [Cu(NH_3)_3(H_2O)_3]^{2+} + H_2O \qquad K_3 = 1 \times 10^3$$
$$[Cu(NH_3)_3(H_2O)_3]^{2+} + NH_3 \rightleftharpoons [Cu(NH_3)_4(H_2O)_2]^{2+} + H_2O \qquad K_4 = 2 \times 10^2$$
$$[Cu(NH_3)_4(H_2O)_2]^{2+} + NH_3 \rightleftharpoons [Cu(NH_3)_5(H_2O)]^{2+} + H_2O \qquad K_5 = 3 \times 10^{-1}$$
$$[Cu(NH_3)_5(H_2O)]^{2+} + NH_3 \rightleftharpoons [Cu(NH_3)_6]^{2+} + H_2O \qquad K_6 = \text{very small}$$

The tetrahedral crystal field

Following Figure shows a convenient way of relating a tetrahedron to a Cartesian axis set.

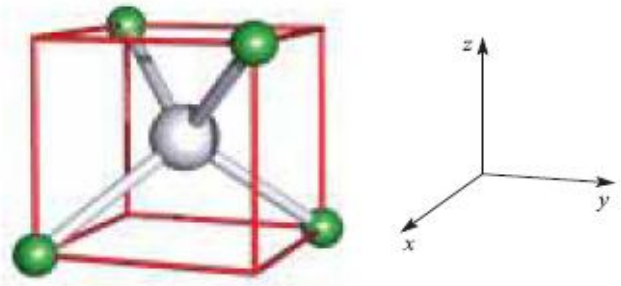

Fig. shows the relationship between a tetrahedral ML_4 complex and a cube; the cube is readily related to a Cartesian axis set. The ligands lie between the x, y and z axes; compare this with an octahedral complex, where the ligands lie on the axes.

With the complex in this orientation, none of the metal **d** orbitals points exactly at the ligands, but the d_{xz}, d_{yz} and d_{xy} orbitals come nearer to doing so than the d_{z2} and d_{x2-y2} orbitals. For a regular tetrahedron, the splitting of the **d** orbitals is inverted

compared with that for a regular octahedral structure, and the energy difference (Δ_{tet}) is smaller. The relative splittings Δ_{oct} and Δ_{tet} are related by following equation.

$$\Delta_{tet} = \frac{4}{9}\Delta_{oct} \cong \frac{1}{2}\Delta_{oct}$$

Following Figure compares crystal field splitting for octahedral and tetrahedral fields; remember, the subscript g in the symmetry labels is not needed in the tetrahedral case.

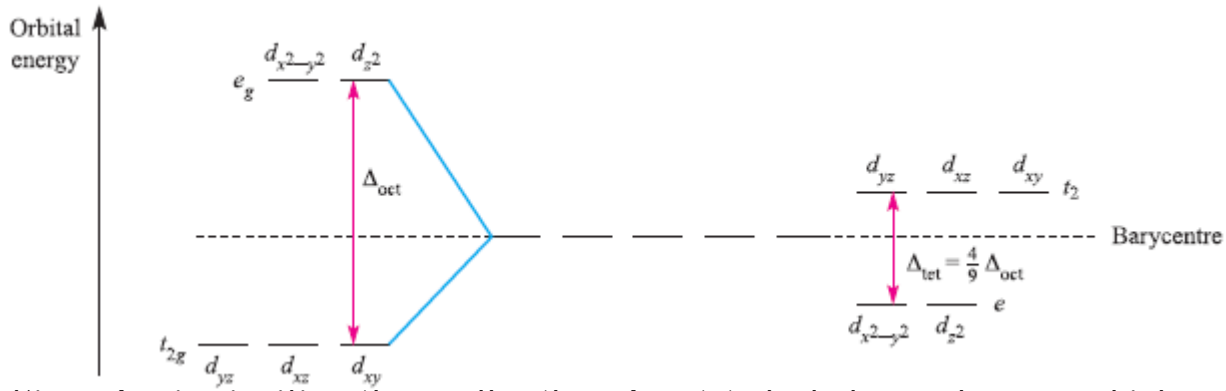

Since Δ_{tet} is significantly smaller than Δ_{oct}, tetrahedral complexes are high-spin. Also, since smaller amounts of energy are needed for e → t_2 transitions (tetrahedral) than for $t_{2g} \rightarrow e_g$ transitions (octahedral), corresponding octahedral and tetrahedral complexes often have different colours.

Tetrahedral complexes are almost invariably high-spin. The effects of a strong field ligand which also lowers the symmetry of the complex can lead to a low-spin 'distorted tetrahedral' system. This is a rare situation, and is observed in some cobalt(II) complexes.

Jahn–Teller effects in tetrahedral complexes are illustrated by distortions in $\mathbf{d^9}$ (e.g. $[CuCl_4]^{2-}$) and high-spin $\mathbf{d^4}$ complexes.

The square planar crystal field

A square planar arrangement of ligands can be formally derived from an octahedral array by removal of two trans ligands. If we remove the ligands lying along the z axis, then the dz^2 orbital is greatly stabilized; the energies of the dyz and d_{xz} orbitals are also lowered as following Figure.

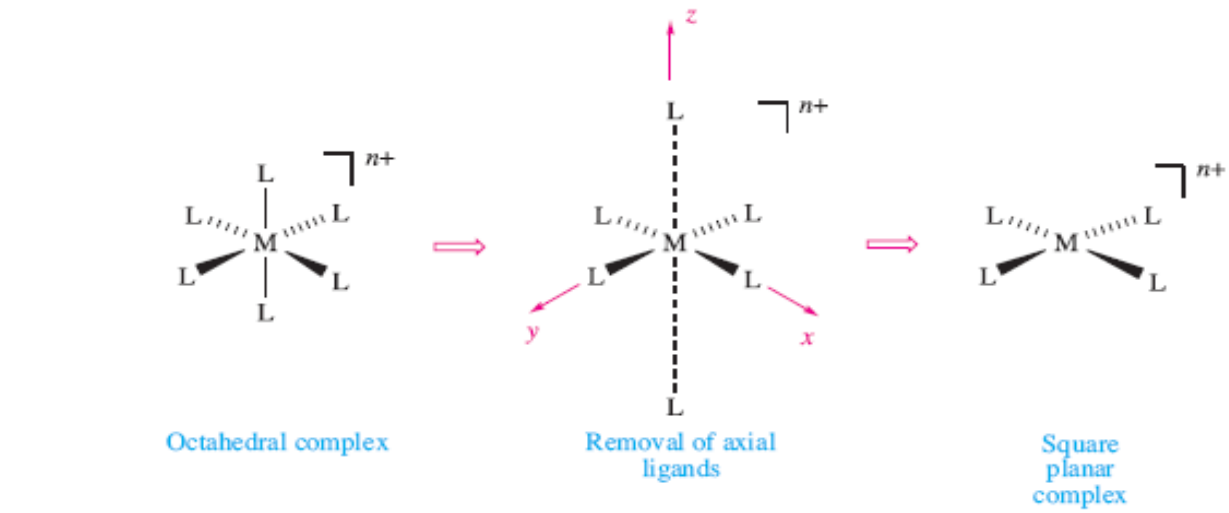

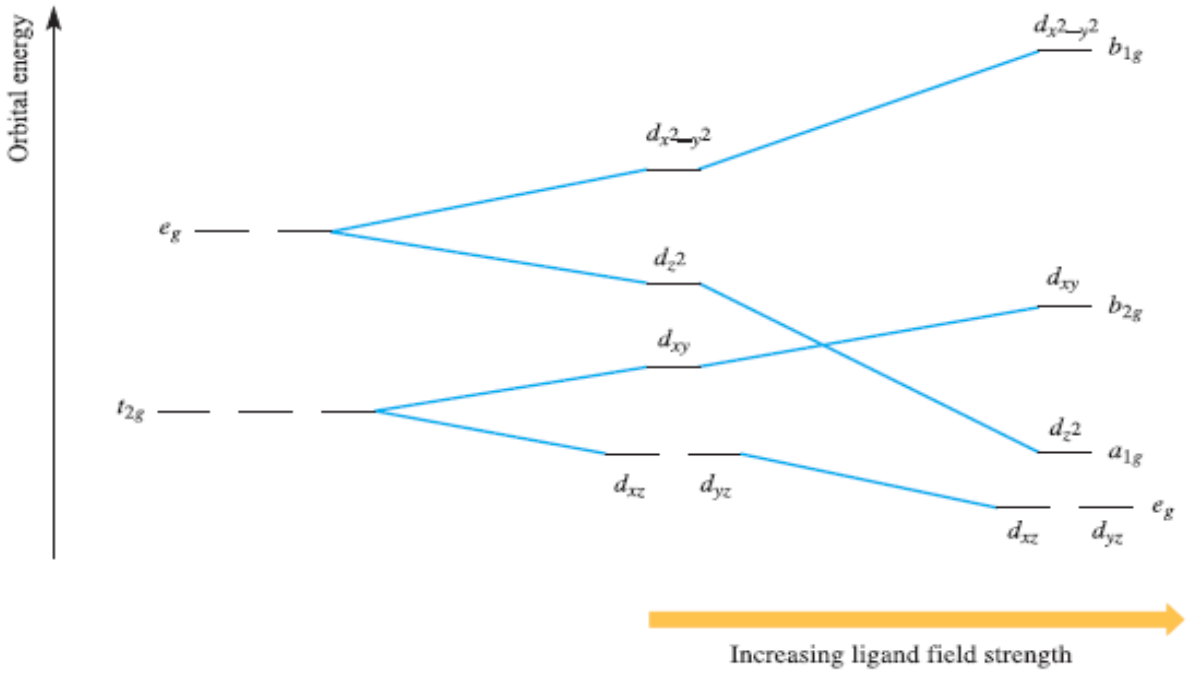

The fact that square planar $\mathbf{d^8}$ complexes such as $[Ni(CN)_4]^{2-}$ are diamagnetic is a consequence of the relatively large energy difference between the d_{xy} and $d_{x2\ -y2}$ orbitals, while $[NiCl)_4]^{2-}$ is paramagnetic is a consequence of the relatively small energy difference between the e_g and t_2 orbitals as shown below.

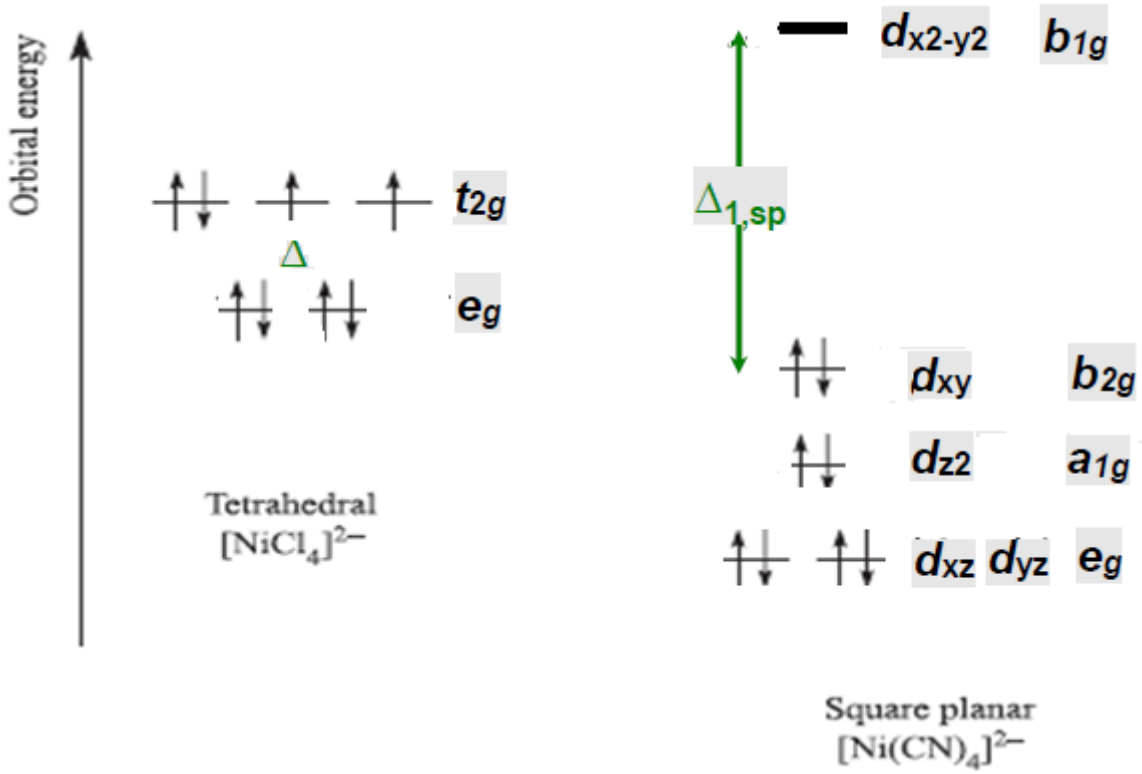

Thus, $[NiCl_4]^{2-}$ is paramagnetic while $[Ni(CN)_4]^{2-}$ is diamagnetic.

Other crystal fields

Figure below shows crystal field splittings for some common geometries with the relative splitting of the **d** orbitals with respect to Δ_{oct}. By using these splitting diagrams, it is possible to rationalize the magnetic properties of a given complex.

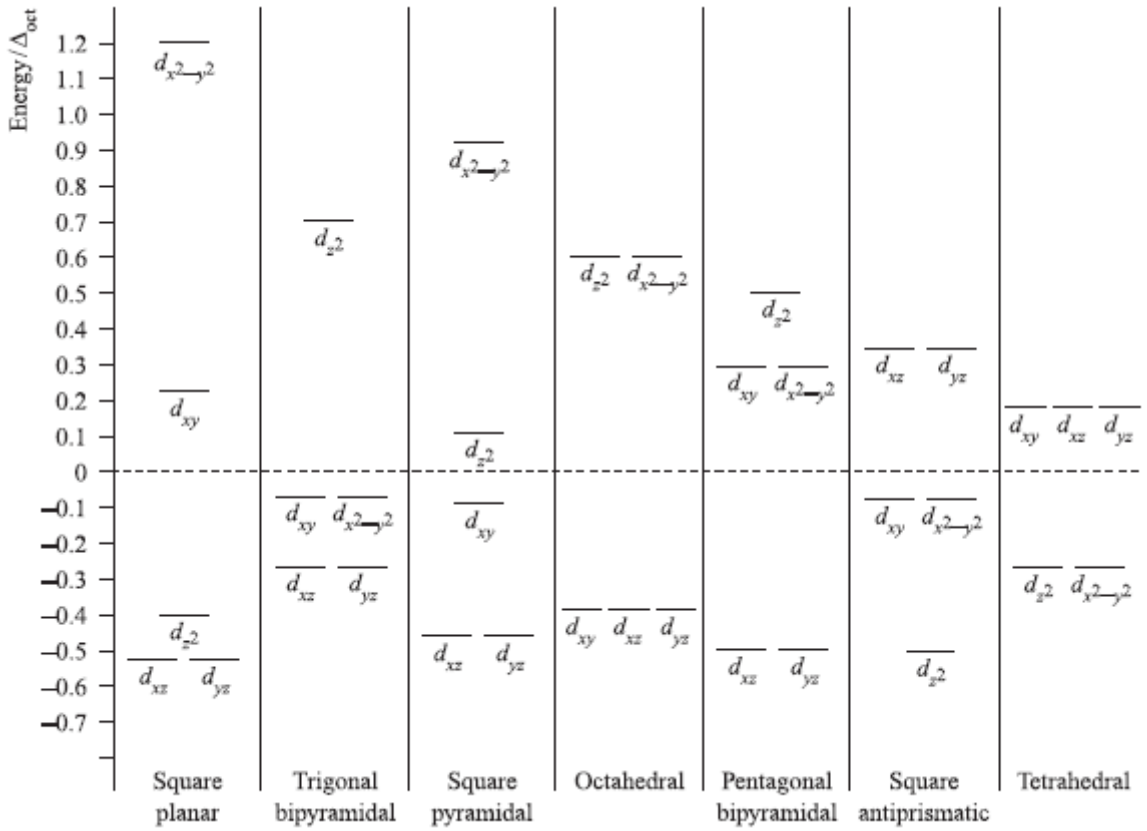

Successes of Crystal Field Theory

A good chemical theory is one that can account for many aspects of physical and chemical behavior. By this standard, crystal field theory is remarkably successful, because it can be used to explain most of the properties that are unique to transition metal ions. Here we will look at a selection of them.

1- Magnetic Properties

Crystal field theory explains the paramagnetism very well in terms of the splitting of the *d*-orbital energies, at least for the Period 4 transition metals. For example, we have just seen how crystal fi eld theory can explain the diamagnetism of the square planar nickel(II) ion, which contrasts with the paramagnetism of the tetrahedral and octahedral geometries. The theoretical degree of paramagnetism is given by the *magnetic moment* of a compound.

This can be calculated using the simple formula $\mu=\sqrt{n(n+2)}$, where *n* is the number of unpaired electrons. The units of magnetic moment are Bohr magnetons, μ_{BM}. Therefore, $[Ti(OH_2)_6]^{3+}$ has 1 unpaired electron and has a magnetic moment of 1.73 μ_{BM}.

2-Colors of Transition Metal Complexes

The most striking feature of transition metal complexes is the range of colors that they exhibit. These colors are the result of absorptions in the visible region of the electromagnetic spectrum. For example, Figure below shows the visible absorption spectrum of the purple hexaaquatitanium(III) ion, $[Ti(OH_2)_6]^{3+}$.

This ion absorbs light in the green part of the spectrum, transmitting blue and red light to give the blended purple color.

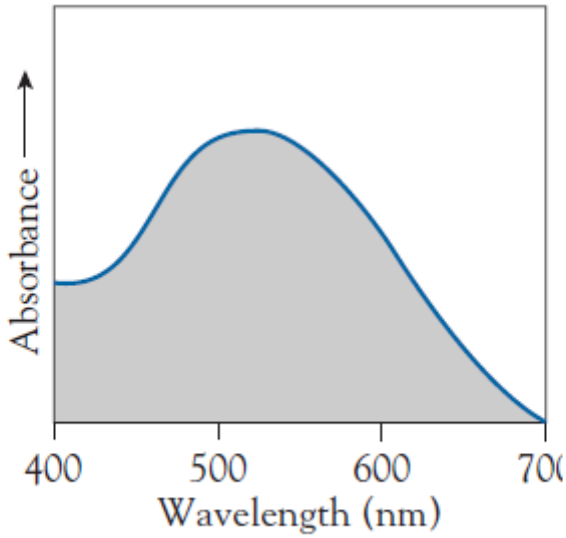

The visible absorption spectrum of the hexaaquatitanium(III) ion.

3- **Hydration Enthalpies**

Another of the parameters that can be explained by crystal field theory is the enthalpy of hydration of transition metal ions. This is the energy released when gaseous ions are hydrated.

$$M^{n+}(g) + 6\,H_2O(l) \rightarrow [M(OH_2)_6]^{n+}(aq)$$

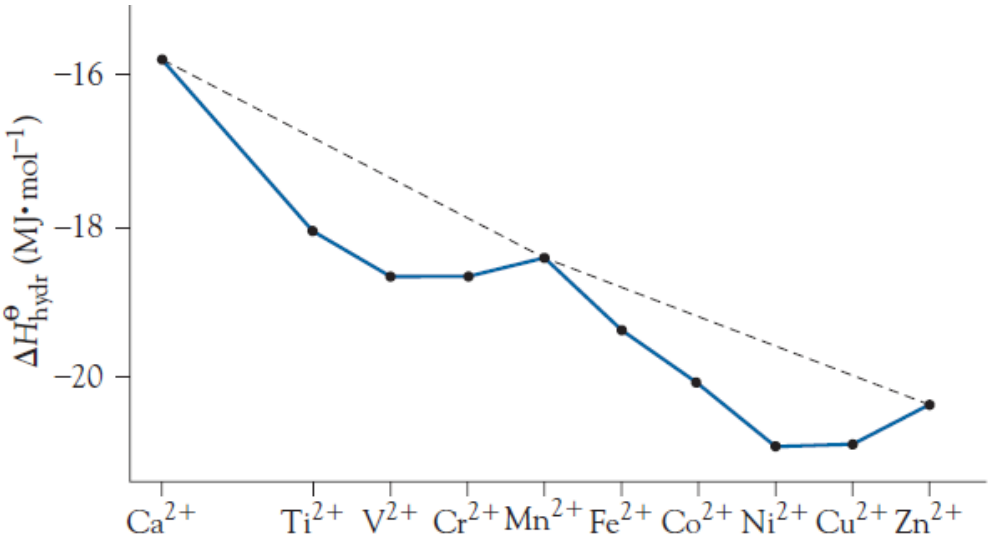

Experimental hydration enthalpies of the dipositive ions of the Period 4 transition metals.

As the effective nuclear charge of metal ions increases across a period, we expect the electrostatic interaction between the water molecules and the metal ions to increase regularly along the transition metal series. In fact, we find deviations from a linear relationship (Figure above). To explain this observation, we assume that the greater hydration enthalpy is the result of the crystal field stabilization energy, which can be calculated in terms of Δ_{oct}, the crystal field splitting. Recall that for an octahedral field, the d_{xy}, d_{xz}, and d_{yz} orbitals are lowered in energy by 2/5 Δ_{oct},and the $d_{x2\text{-}y2}$ and d_{z2} orbitals are raised in energy by 3/5 Δ_{oct}. Thus, for a particular electron configuration, it is possible to calculate the net contribution of the crystal field to the hydration enthalpy. Figure below illustrates the situation for the d^4 high-spin ion. This ion would have a net stabilization energy of:

$$-[3(\tfrac{2}{5}\Delta_{oct})]+[1(\tfrac{3}{5}\Delta_{oct})]=-0.6\Delta_{oct}$$

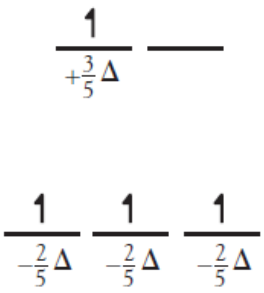

The crystal field stabilization energy for the d^4 high-spin electron configuration.

Crystal field stabilization energies (CFSE) for the dipositive, high-spin ions of various Period 4 metals

Ion	Configuration	CFSE
Ca^{2+}	d^0	$-0.0\ \Delta_{oct}$
—	d^1	$-0.4\ \Delta_{oct}$
Ti^{2+}	d^2	$-0.8\ \Delta_{oct}$
V^{2+}	d^3	$-1.2\ \Delta_{oct}$
Cr^{2+}	d^4	$-0.6\ \Delta_{oct}$
Mn^{2+}	d^5	$-0.0\ \Delta_{oct}$
Fe^{2+}	d^6	$-0.4\ \Delta_{oct}$
Co^{2+}	d^7	$-0.8\ \Delta_{oct}$
Ni^{2+}	d^8	$-1.2\ \Delta_{oct}$
Cu^{2+}	d^9	$-0.6\ \Delta_{oct}$
Zn^{2+}	d^{10}	$-0.0\ \Delta_{oct}$

The complete set of crystal field stabilization energies is listed in Table above. These values correspond remarkably well with the deviations of the hydration enthalpies. Of particular note, it is only the d^0, d^5 (high spin), and d^{10} ions that fit the expected near-linear relationship, and these all have zero crystal field stabilization energy.

4-Spinel Structures

The spinel is a mixed oxide, usually of general formula $(M^{2+})(M^{3+})_2(O^{2-})_4$, with the metal ions occupying both octahedral and tetrahedral sites. In a **normal spinel**, all of the 2+ ions are in the tetrahedral sites and the 3+ ions are in the octahedral sites, whereas in an **inverse spinel**, the 2+ ions are in the octahedral sites and the 3+ ions fill the tetrahedral sites and the remaining octahedral sites.

The choice of normal spinel or inverse spinel for mixed transition metal oxides is determined usually (but not always) by which option will give the greater crystal field stabilization energy. This can be illustrated by a pair of oxides each of which contains ions of one metal in two different oxidation states:

Fe_3O_4, containing Fe^{2+} and Fe^{3+}, and Mn_3O_4, containing Mn^{2+} and Mn^{3+}. The former adopts the inverse spinel structure: $(Fe^{3+})_t(Fe^{2+}, Fe^{3+})_o(O^{2-})_4$. All these ions are high spin, so the Fe^{3+} ion (d^5) has a zero CFSE, but the Fe^{2+} ion (d^6) has a nonzero CFSE. Because a crystal field splitting for the tetrahedral geometry is four-ninths that of the equivalent octahedral environment, the CFSE of an octahedrally coordinated ion will be greater than that of a tetrahedrally coordinated ion. This energy difference accounts for the octahedral site preference of the Fe^{2+} ion. Unlike the mixed iron oxide, the mixed manganese oxide has the normal spinel structure: $(Mn^{2+})_t(Mn^{3+})_o(O^{2-})_4$. In this case, it is the Mn^{2+} ion (d^5) that has a zero CFSE and the Mn^{3+} ion (d^4) that has a nonzero CFSE. Hence, it is the Mn^{3+} ion that preferentially occupies the octahedral sites.

Notes

Structure of Normal Spinels (AB_2O_4): The divalent A^{II} ions occupy the tetrahedral voids, whereas the trivalent B^{III} ions occupy the octahedral voids in the close packed arrangement of oxide ions.

A normal spinel can be represented as: $\mathbf{(A^{II})^{tet}(B^{III})_2{}^{oct}O_4}$

E.g. $MgAl_2O_4$ (known as spinel), Mn_3O_4, $ZnFe_2O_4$, $FeCr_2O_4$ (chromite) etc.

Structures of Inverse spinels ($B(AB)O_4$): The A^{II} ions occupy the octahedral voids, whereas half of B^{III} ions occupy the tetrahedral voids. It can be represented as: $(B^{III})^{tet}(A^{II}B^{III})^{oct}O_4$

E.g. Fe_3O_4 (ferrite), $CoFe_2O_4$, $NiFe_2O_4$ etc.

The above inverse spinels can also be written as:

$Fe_3O_4 = Fe^{III}(Fe^{II}Fe^{III})O_4$

$CoFe_2O_4 = Fe^{III}(Co^{II}Fe^{III})O_4$

$NiFe_2O_4 = Fe^{III}(Ni^{II}Fe^{III})O_4$

The number of octahedral sites occupied may be ordered or random. The random occupation leads to defected spinels.

E.g. $NiAl_2O_4$ for which the formula can be written as $(Al_{0.75}Ni_{0.25})^{tet}\ [Ni_{0.75}Al_{1.25}]^{octa}O_4$.

Another defected spinel is γ-Al_2O_3

Some Generalizations Regarding The Structures Of Spinels

* A normal spinel structure is assumed if both the divalent and the trivalent metals are non transition metals since no CFSE is involved.

* There is a tendency of formation of inverse spinel structure in some cases (not all the cases) which contain transition metal ions. This is because, the transition metal ion may get extra stability (LFSE) in octahedral geometry, prefers octahedral voids over tetrahedral ones.

* The d^0; high spin d^5, d^{10} ions have no preference between tetrahedral and octahedral coordination since the LFSE is zero.

* Usually d^3 & d^8 ions have strongest preference for octahedral geometry.

* Other ions with d^1, d^2, d^4, d^6, d^7, d^9 too have slightly more preference for octahedral symmetry.

* That means, if A^{II} has d^3 or d^8 configuration and the B^{III} ion has configuration other than these, then the spinel is inverted.

* If the divalent A^{II} is a transition metal (with configurations other than d^0; highspin d^5 & d^{10}) and the B^{III} ion is a non transition metal, there is a tendency to form inverse spinel.

But there are exceptions like $FeAl_2O_4$ which has normal spinel structure.

* Above generalizations are valid for high spin systems as the oxide ion is expected to be a weak field ligand.

For example, Co^{3+} is a low spin system even in presence of oxo ligands due to high charge on the ion.

A^{II}	**B^{III}**	**Structure**
Non transition metal or d^0 or d^5 or d^{10} transition metal	Non transition metal	Spinel structure
Non transition metal or d^0 or d^5 or d^{10} transition metal	A transition metal with d^1 or d^2 or d^3 or d^4 or d^6 or d^7 or d^8 or d^9 configurations	Spinel structure
A transition metal with d^1 or d^2 or d^3 or d^4 or d^6 or d^7 or d^8 or d^9 configurations	Non transition metal or transition meta with d^0 or d^5 or d^{10} configurations	Inverse spinel
Transition metal with higher CFSE value	Transition metal with lower CFSE value	Inverse spinel

Examples For Spinel And Inverse Spinel Structures

1) **$MgAl_2O_4$ is a normal spinel** since both the divalent and trivalent ions are non transition metal ions. There is no question of CFSE.

2) **Mn_3O_4 is a normal spinel** since the Mn^{2+} ion is a high spin d^5 system with zero LFSE. Whereas, Mn^{3+} ion is a high spin d^4 system with considerable LFSE.

3) **Fe_3O_4 is an inverse spinel** since the Fe(III) ion is a high spin d^5 system with zero CFSE. Whereas the divalent Fe(II) is a high spin d^6 system with more CFSE.

4) **$NiFe_2O_4$ is again an inverse spinel** since the divalent Ni^{2+} (a d^8 ion) has more CFSE than the trivalent Fe^{3+} (a d^5 ion).

5) **$FeCr_2O_4$ is a normal spinel** since the divalent Fe^{2+} is a high spin d^6 ion with CFSE = 4 Dq and the trivalent Cr^{3+} is a high spin d^3 ion with CFSE = 12 Dq. Hence Cr^{3+} gets more OSSE while occupying octahedral sites.

6) **Co_3O_4 is a normal spinel**. Even in the presence of weak field oxo ligands, the Co^{3+} is a low spin d^6 ion with very high CFSE. It is due to high charge on Co^{3+}. Hence all the Co^{3+} ions occupy the octahedral sites.

7) **$NiAl_2O_4$ show random or defected inverse spinel**. The CFSE of Ni^{II} is greater in octahedral than tetrahedral coordination. But Al^{3+} also has strong preference for octahedral sites due to high lattice energy. This leads to almost complete randomization of all the cations on all the available sites. Its formula can be written as $(Al_{0.75}Ni_{0.25})^{tet}\,[Ni_{0.75}Al_{1.25}]^{octa}O_4$.

Molecular Orbital Theory (MOT)

In this section, There are another approach to the bonding in metal complexes: the use of molecular orbital theory (MOT). In contrast to crystal field theory, the molecular orbital model considers covalent interactions between the metal centre and ligands.

Octahedral Complexes

For octahedral complexes, the molecular orbitals can be described as resulting from a combination of a central metal atom accepting a pair of electrons from each of six ***σ*-donor** ligands. The interaction of these ligands with of the metal ***s, p*** and ***d*** orbitals is shown in following.

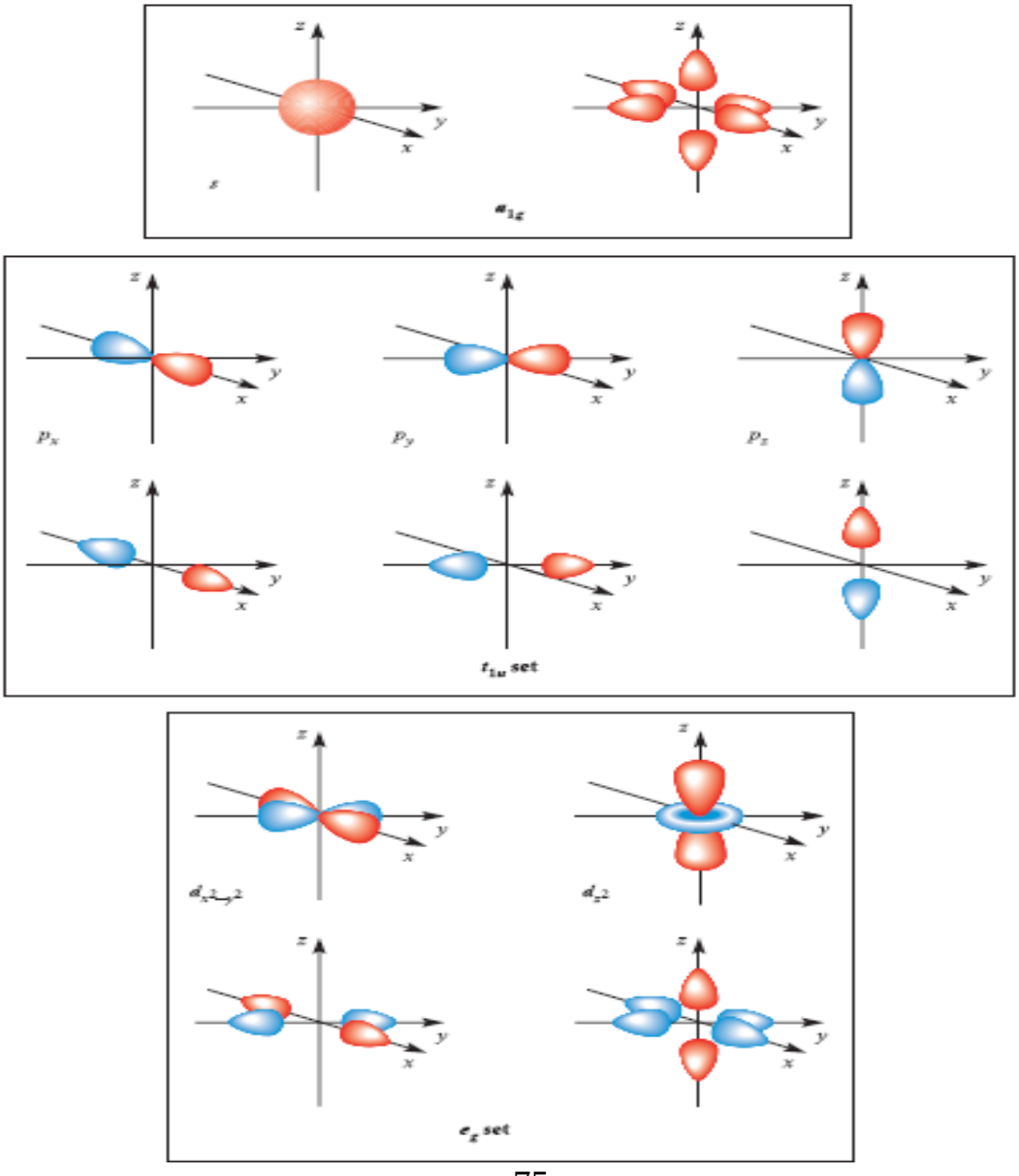

The ***s*** orbital has **a_1g** symmetry, the ***p*** orbitals are degenerate with ***t_1u*** symmetry, and the ***d*** orbitals split into two sets with **eg** (dz^2 and dx^2 -y^2 orbitals) and **t_2g** (dxy, dyz and dxz orbitals) symmetries, respectively.

Each ligand, **L**, provides one orbital and derivation of the ligand group orbitals(LGOs) for the O_h L_6 fragment. These LGOs have **a_1g**, **t_1u** and **eg** symmetries. Symmetry matching between metal orbitals and LGOs allows the construction of the MO diagram shown in following Figure .

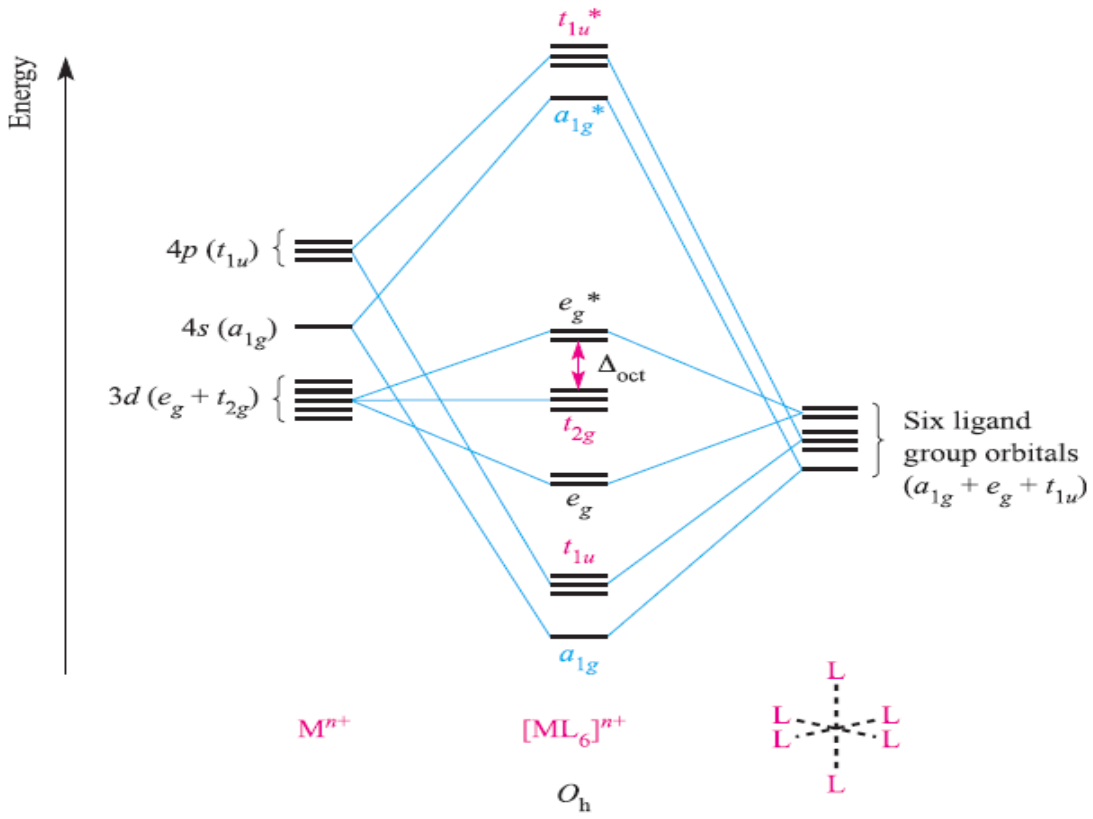

Combinations of the metal and ligand orbitals generate six bonding and six antibonding molecular orbitals. The metal dxy, dyz and dxz atomic orbitals have **t_2g** symmetry and are non-bonding (as shown in Figure above). The overlap between the ligand and metal ***s*** and ***p*** orbitals is greater than that involving the metal ***d*** orbitals, and so the **a_1g** and **t_1u** MOs are stabilized to a greater extent than the **eg** MOs.

In an octahedral complex with no π-bonding. i.e. have **σ-bonding only**, the energy difference between the **t_2g** and **eg** levels corresponds to Δ_{oct} in crystal field theory.

The MO diagram of octahedral of **σ-bonded** complexes can be represented in examples:

1- In low-spin $[Co(NH_3)_6]^{3+}$, 18 electrons (six from Co^{3+} and two from each ligand) occupy the **a_1g, t_1u, eg** and **t_2g** MOs;

2- In high-spin $[CoF_6]^{3-}$, 18 electrons are available, 12 occupying the **a_1g**, **t_1u** and **eg** MOs, four the **t_2g** level, and two the **eg^*** level. Whether a complex is high- or low-spin depends upon the energy separation of the **t_2g** and **eg** levels.

Notionally, in a σ-bonded octahedral complex, the 12 electrons supplied by the ligands are considered to occupy the **a_1g**, **t_1u** and **eg** orbitals. Occupancy of the **t_2g** and **eg** levels corresponds to the number of valence electrons of the metal ion, just as in crystal field theory. The molecular orbital model of bonding in octahedral complexes gives much the same results as crystal field theory. It is when we move to complexes with M-L π-bonding that distinctions between the models emerge.

Complexes with metal-ligand π bonding

The metal dxy, dyz and dxz atomic orbitals (the **t_2g** set) are nonbonding in an $[ML_6]^{n+}$, σ-bonded complex (Figure above) and these orbitals may overlap with ligand orbitals of the correct symmetry to give π-interactions as following Figure.

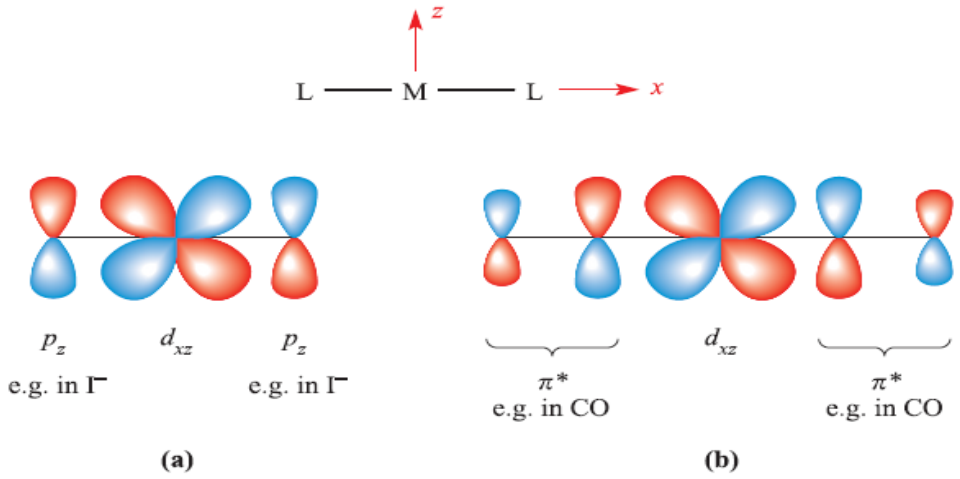

Although π-bonding between metal and ligand ***d*** orbitals is sometimes considered for interactions between metals and phosphine ligands (e.g. PR_3 or PF_3), it is more realistic to consider the roles of ligand σ*-orbitals as the acceptor orbitals. Two types of ligand must be differentiated: **π-donor** and **π-acceptor** ligands.

A **π-donor** ligand donates electrons to the metal centre in an interaction that involves a filled ligand orbital and an empty metal orbital; a **π-acceptor** ligand accepts electrons from the metal centre in an interaction that involves a filled metal orbital and an empty ligand orbital.

π-donor ligands include Cl^-, Br^- and I^- and the metal– ligand π-interaction involves transfer of electrons from filled ligand ***p*** orbitals to the metal centre Figure **(a)**. Figure (**a)** shows the interaction between a metal ion and six **π-donor** ligands; electrons are omitted from the diagram. The ligand group π-orbitals are filled and lie above, but relatively close to, the ligand σ-orbitals, and interaction with the metal

dxy, dyz and dxz atomic orbitals leads to bonding (t_2g) and antibonding (t_2g^*) MOs. The energy separation between the **t_2g** and **eg** levels corresponds to Δ_{oct}.

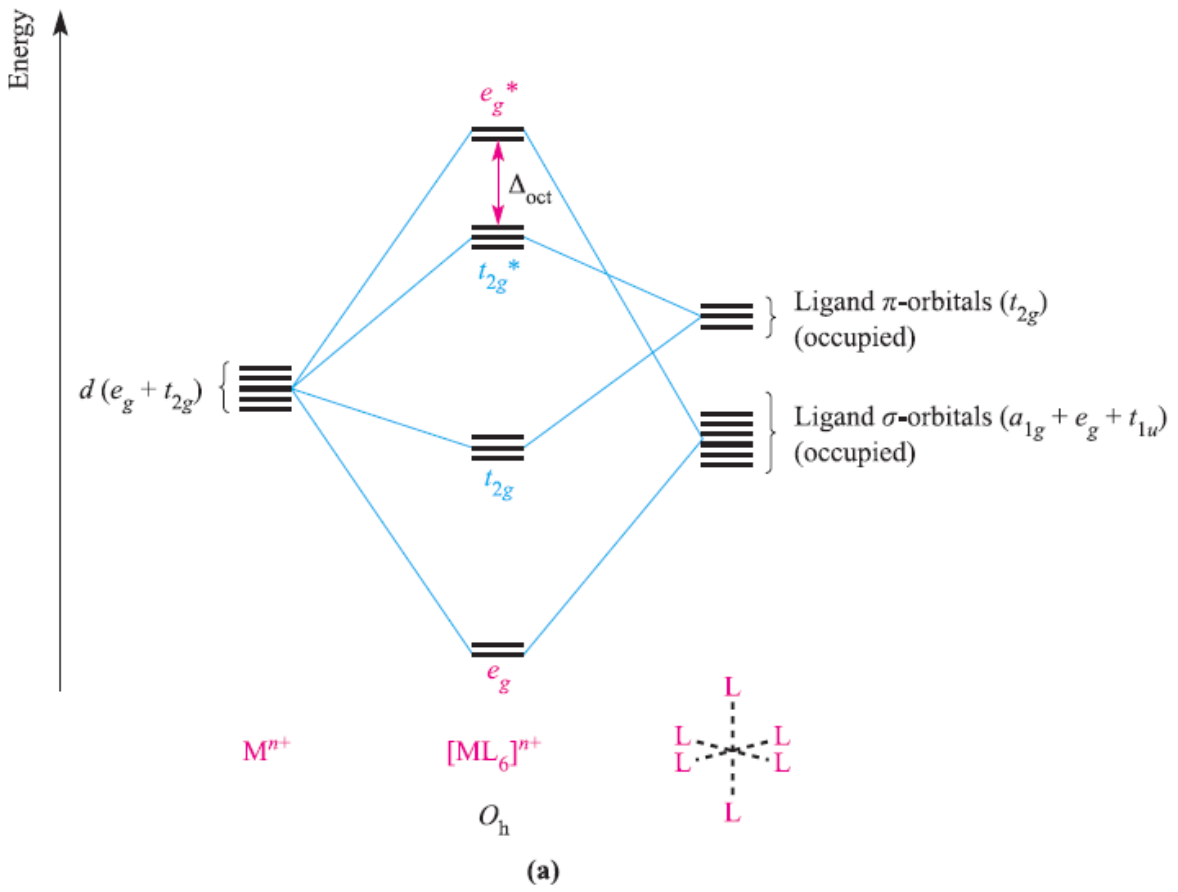

Figure **b** shows the interaction between a metal ion and six **π-acceptor** ligands. The vacant ligand π*-orbitals lie significantly higher in energy than the ligand σ-orbitals. Examples of **π-acceptor** ligands are CO, N_2, NO and alkenes, and the metal–ligand π-bonds arise from the ***back-donation*** of electrons from the metal centre to vacant antibonding orbitals on the ligand. **π-Acceptor** ligands can stabilize low oxidation state metal complexes.

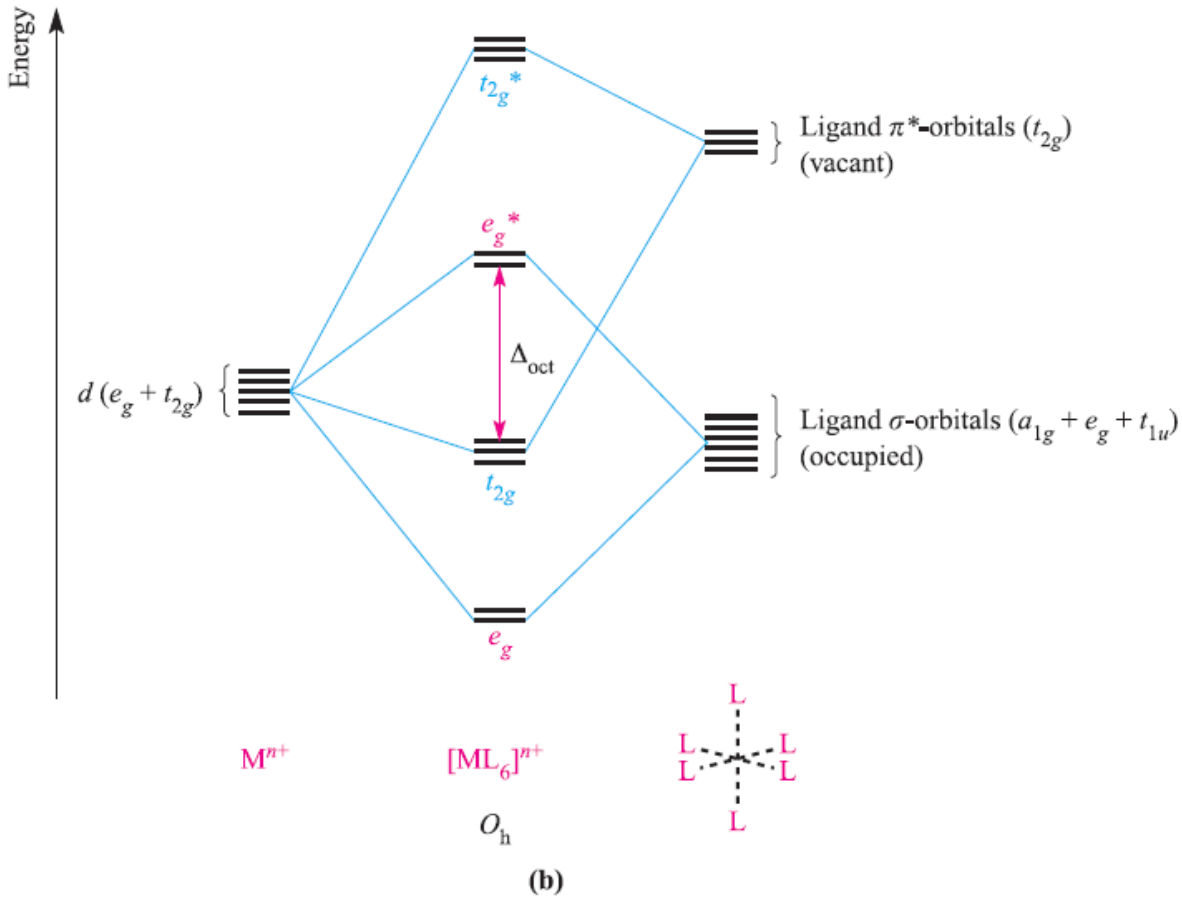

Tetrahedral Complexes

Sigma bonding

The energy level picture for the d orbitals is inverted from the octahedral levels, with **e** the nonbonding and ***t₂*** the bonding and antibonding levels(Figure below). In addition, the split (now called Δ_{tet},) is smaller than for octahedral geometry; the general result is:

$$\Delta_{tet} = \frac{4}{9}\Delta_{oct} \cong \frac{1}{2}\Delta_{oct}$$

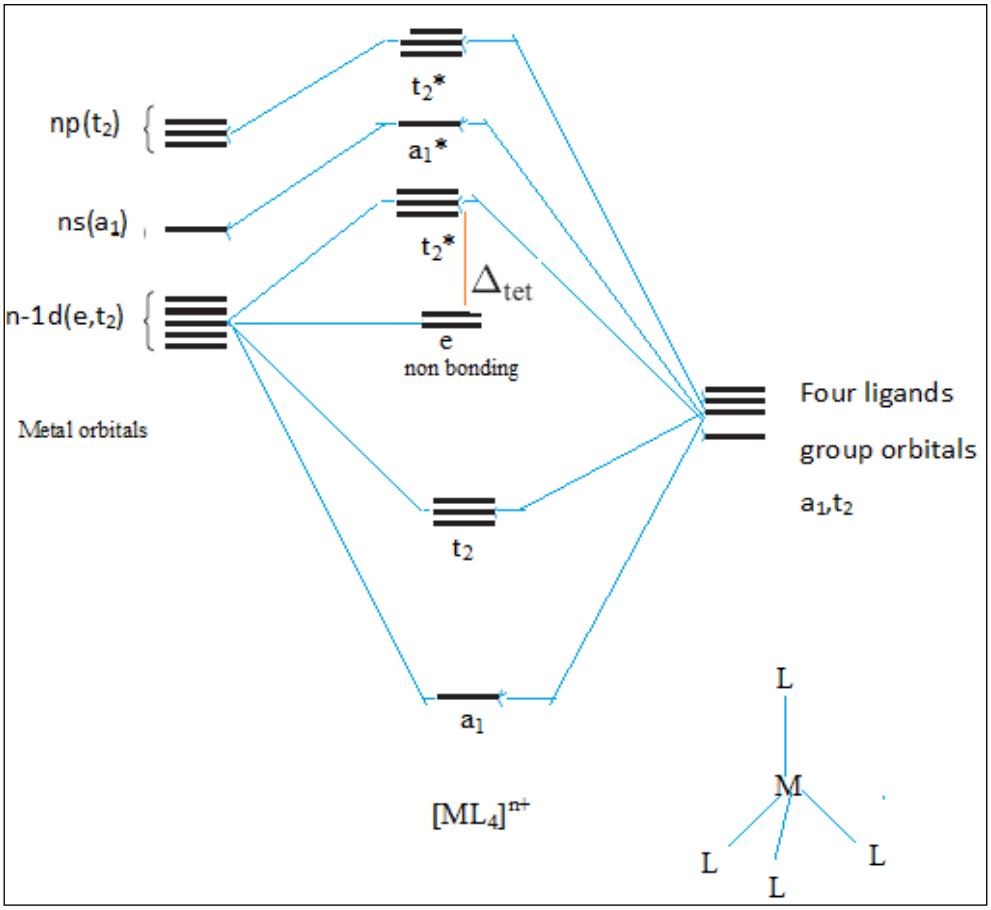

Pi bonding

The reducible representation includes the ***E,*** ***T1,*** and ***T2*** irreducible representations. The ***T1*** has no matching metal atom orbitals, ***E*** matches dZ^2 and dX^2-y^2, and ***T2*** matches *dxy*, *dxz*, and *dyz*. The E and T_2 interactions lower the energy of the bonding orbitals, and raise the corresponding antibonding orbitals, for a net increase in Δ_{tet}. An additional complication appears when both bonding and antibonding π orbitals are available on the ligand, as is true for CO or CN^-. Following Figure shows the orbitals and their relative energies for $Ni(CO)_4$, in which the interactions of the CO ***σ*** and π orbitals with the metal orbitals are probably small.

Much of the bonding is from M → L π bonding. In cases in which the ***d*** orbitals are not fully occupied, ***σ*** bonding is likely to be more important, with resulting shifts

of the a_1 and t_2 orbitals to lower energies and the **4s** and **4p** orbitals to higher energies.

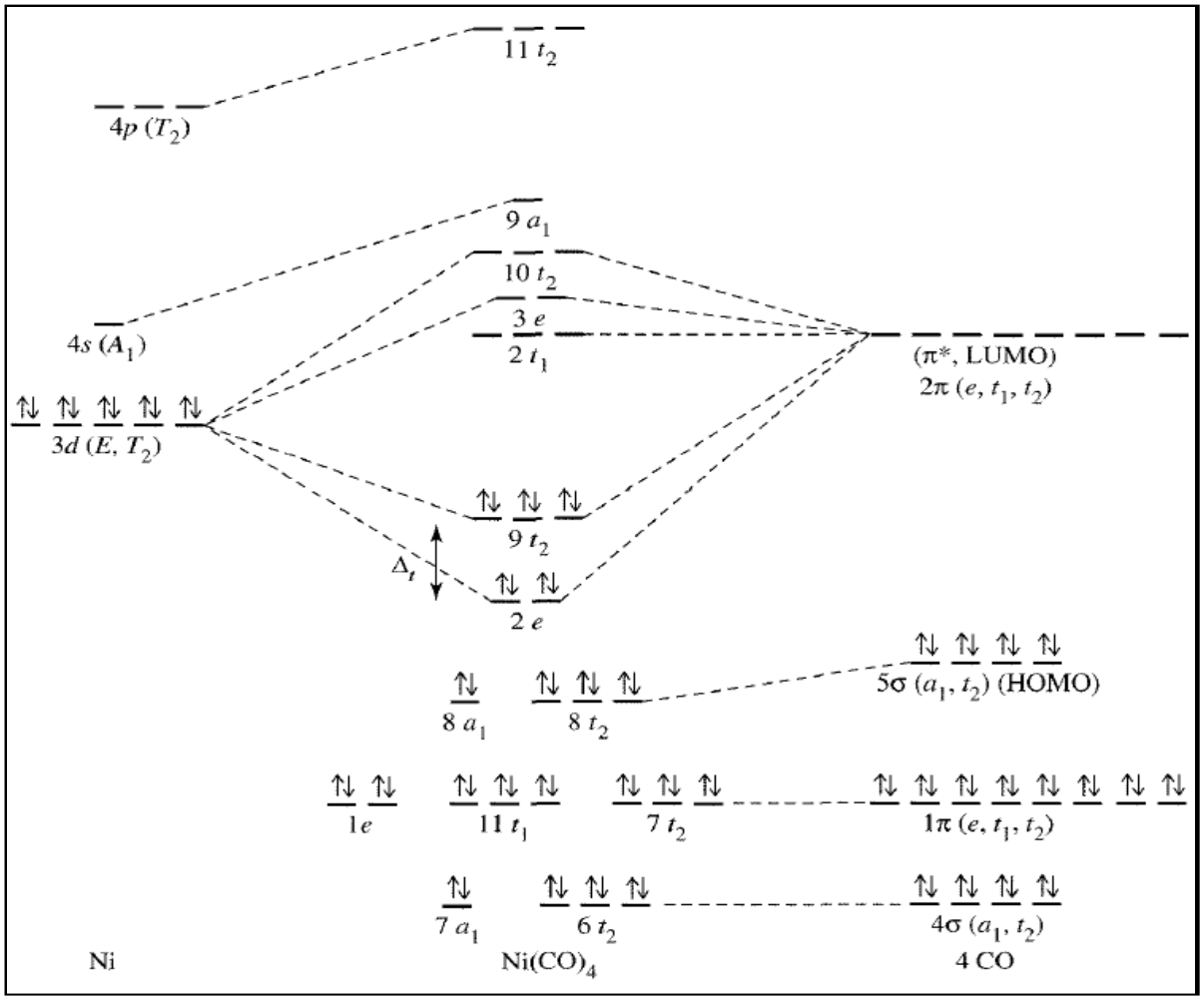

Square planar complxes

In D_{4h} symmetry of the square planar complxes such as $PdCl_4^{=}$ the *d* orbitals are split into the b_{1g} (d_{x2-y2}), b_{2g} (d_{xy}), a_{1g} (d_{z2}), and *eg* (d_{xz} and d_{yz}) subsets. The p_x and p_y orbitals point directly at ligands and in D_{4h} symmetry they constitute an e_u set. The p_z orbital has a_{2u} symmetry, and the four σ orbitals from the ligands give a_{1g} , e_u , and b_{1g} symmetry. Therefore, the b_{2g} , e_g , and a_{2u} behave as nonbonding orbitals.
When we consider the four ligands lying on the *x* and *y* axes (as shown in Figure below), it becomes apparent that the d_{x2-y2} orbital has positive lobes along the *x* -axis and negative lobes along the *y* -axis.

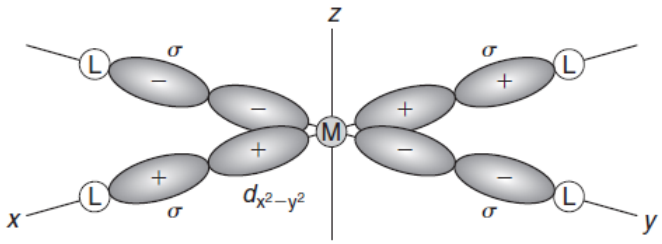

The combinations of metal and ligand orbitals in a square planar complex. Although not shown, the p_x and p_y orbitals are directed toward the ligands in the same way as are the lobes of the $d_{x^2-y^2}$ orbital. The *p* orbitals have positive and negative lobes along *each* axis rather than positive on the *x*-axis and negative on the *y*-axis as in the case of the $d_{x^2-y^2}$ orbital.

The molecular orbitals give rise to the energy level diagram shown in Figure below. From the molecular orbital energy level diagram shown in this figure, it can be seen that the orbitals designated as e_g , a_{1g} , and b_{1g}* correspond to the d_{xz} , d_{yz} , d_{z2} , and d_{xy} orbitals in the ligand field diagram shown in Figure below . In the ligand field model, Δ represented the difference in energy between the d_{xy} and the d_{x2-y2} orbitals. In the molecular orbital model, Δ represents the difference in energy between the e_g and a_{1g} orbitals.

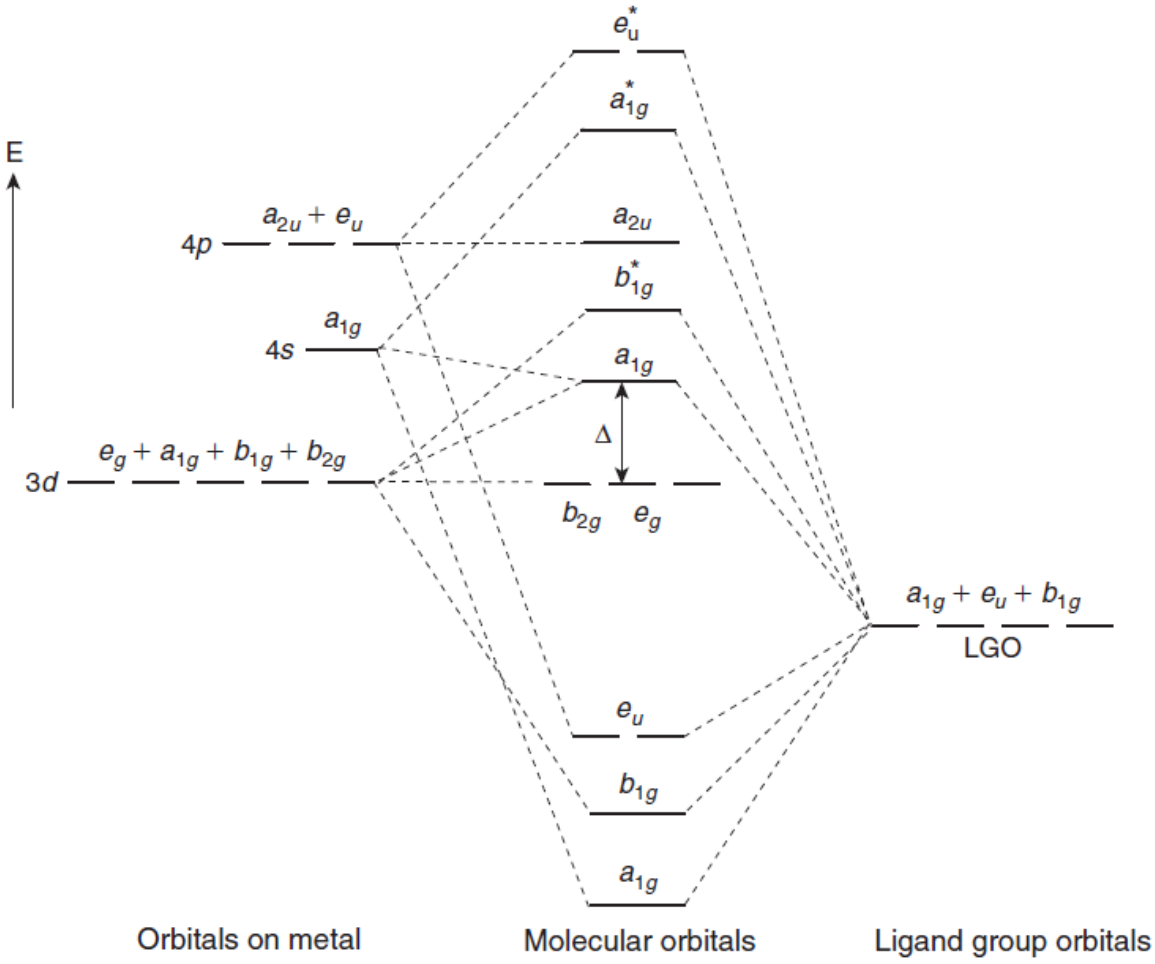

A molecular orbital energy level diagram for a square planar complex.

Electronic spectra

A characteristic feature of many d-block metal complexes is their colours, which arise because they absorb light in the visible region (see Figure below).

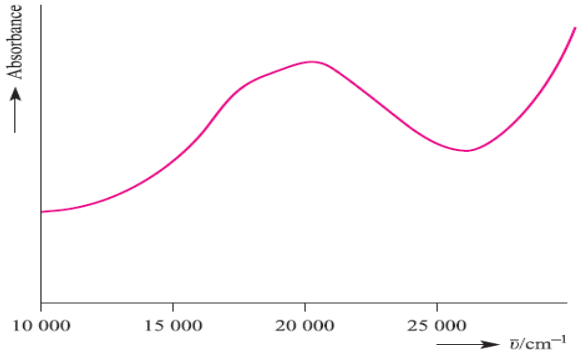

Fig. Shows the electronic spectrum of $[Ti(OH_2)_6]^{3+}$ in aqueous solution.

Studies of electronic spectra of metal complexes provide information about structure and bonding, although interpretation of the spectra is not always straightforward. Absorptions arise from transitions between electronic energy levels:

1) Transitions between metal-centred orbitals possessing d-character (‘**d–d’ transitions**).
2) Transitions between metal- and ligand-centred MOs which transfer charge from metal to ligand or ligand to metal (**charge transfer bands**).

Absorption bands in the electronic spectra of d-block metal compounds are usually broad. The broadness is a consequence of the Franck–Condon approximation which states that electronic transitions are very much faster than nuclear motion (because nuclear mass is far greater than electron mass).

The absorption of a photon of light occurs at ~10^{-18} s whereas molecular vibrations and rotations occur much more slowly. As molecules are vibrating, an electronic transition is essentially a snapshot at a particular set of internuclear distances. It follows that the electronic spectrum will record a range of energies.

Absorption bands are described in terms of λ_{max} corresponding to the absorption maximum A_{max} (see Figure below). The wavelength, λ_{max}, is usually given in nm, but the position of the absorption may also be reported in terms of wavenumbers, $\bar{\upsilon}$ (cm^{-1}). The molar extinction coefficient (or molar absorptivity) ε_{max} of an absorption must also be quoted; ε_{max} indicates how intense an absorption is and is related to A_{max} by following equation where c is the concentration of the solution and ℓ is the pathlength (in cm) of the spectrometer cell.

$$\varepsilon_{max} = \frac{A_{max}}{c \times \ell} \qquad (\varepsilon_{max} \text{ in } dm^3\ mol^{-1}\ cm^{-1})$$

Values of ε_{max} range from close to zero(a very weak absorption) to >10 000dm^3 mol^{-1} cm^{-1} (an intense absorption).

$$\bar{\nu} = \frac{1}{\lambda} = \frac{\nu}{c}$$

400nm corresponds to 25000 cm^{-1}; 200nm corresponds to 50000 cm^{-1}: (nm cm^{1-} $=10^7$)

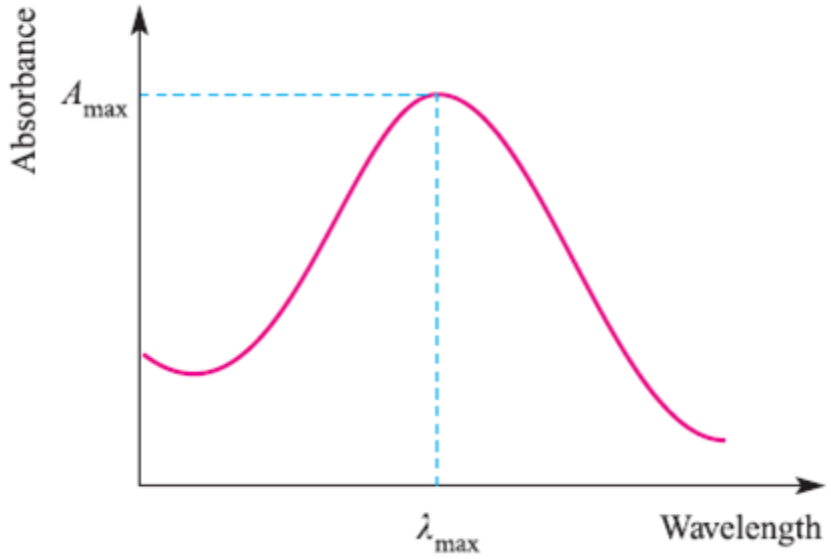

Absorptions in the electronic spectrum of a molecule or molecular ion are often broad, and cover a range of wavelengths. The absorption is characterized by values of _λ_{max} and ε_{max}

Some important points are that the electronic spectra of:

1) d^1, d^4, d^6 and d^9 complexes consist of one broad absorption;
2) d^2, d^3, d^7 and d^8 complexes consist of three broad absorptions;
3) d^5 complexes consist of a series of very weak, relatively sharp absorptions.

Charge transfer absorptions

In metal complexes, intense absorptions (typically in the UV or visible part of the electronic spectrum) may arise from ligand-centred n–π* or π– π* transitions, or from the transfer of electronic charge between ligand and metal orbitals.

The latter fall into two categories:

1) Transfer of an electron from an orbital with primarily ligand character to one with primarily metal character (ligand-to-metal charge transfer, **LMCT**).
2) Transfer of an electron from an orbital with primarily metal character to one with primarily ligand character (metal-to-ligand charge transfer, **MLCT**).

Charge transfer transitions are not restricted by the selection rules that govern 'd–d ' transitions (see later). The probability of these electronic transitions is therefore high, and the absorption bands are therefore intense (Table below).

Table:Typical ε_{max} values for electronic absorptions; a large "max corresponds to an intense absorption and, if the absorption is in the visible region, a highly coloured complex.

Type of transition	Typical ε_{max} / $dm^3\,mol^{-1}\,cm^{-1}$	Example
Spin-forbidden '*d–d*'	<1	$[Mn(OH_2)_6]^{2+}$ (high-spin d^5)
Laporte-forbidden, spin-allowed '*d–d*'	1–10	Centrosymmetric complexes, e.g. $[Ti(OH_2)_6]^{3+}$ (d^1)
	10–1000	Non-centrosymmetric complexes, e.g. $[NiCl_4]^{2-}$
Charge transfer (fully allowed)	1000–50 000	$[MnO_4]^-$

Since electron transfer from metal to ligand corresponds to metal oxidation and ligand reduction, an MLCT transition occurs when a ligand that is easily reduced is bound to a metal centre that is readily oxidized. Conversely, LMCT occurs when a

ligand that is easily oxidized is bound to a metal centre (usually one in a high oxidation state) that is readily reduced. There is, therefore, a correlation between the energies of charge transfer absorptions and the electrochemical properties of metals and ligands.

Ligand-to-metal charge transfer may give rise to absorptions in the UV or visible region of the electronic spectrum. One of the most well-known examples is observed for $KMnO_4$. The deep purple colour of aqueous solutions of $KMnO_4$ arises from an intense LMCT absorption in the visible part of the spectrum as following Figure:

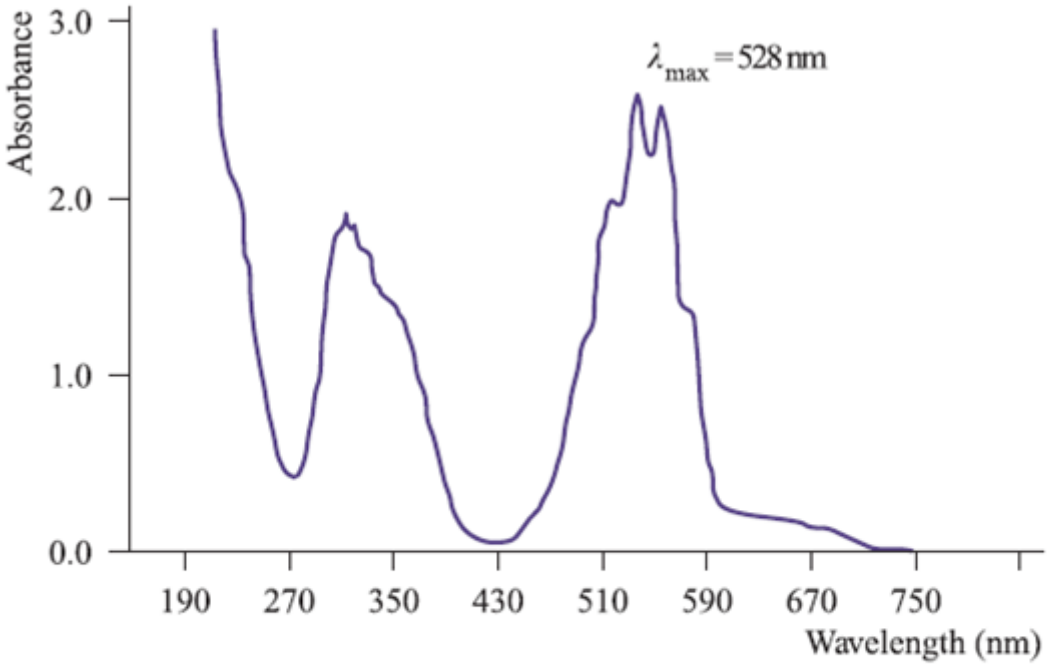

Fig. Part of the electronic spectrum of an aqueous solution of $KMnO_4$. Both absorptions arise from LMCT, but it is the band at 528 nm that gives rise to observed purple colour. Very dilute solutions (here, 1.55×10^{-3} mol dm^{-3}) must be used so that the absorptions remain within the absorption scale.

This transition corresponds to the promotion of an electron from an orbital that is mainly oxygen lone pair in character to a low-lying, mainly Mn-centred orbital. The

following series of complexes illustrate the effects of the metal, ligand and oxidation state of the metal on the position (λ_{max}) of the LMCT band:

- $[MnO_4]^-$ (528 nm), $[TcO_4]^-$ (286 nm), $[ReO_4]^-$ (227 nm);
- $[CrO_4]^{2-}$ (373 nm), $[MoO_4]^{2-}$ (225 nm), $[WO_4]^{2-}$ (199 nm);
- $[FeCl_4]^{2-}$ (220 nm), $[FeBr_4]^{2-}$ (244 nm);
- $[OsCl_6]^{3-}$ (282 nm), $[OsCl_6]^{2-}$ (370 nm).

Across the first two series above, the LMCT band moves to lower wavelength (higher energy) as the metal centre becomes harder to reduce. The values of the absorption maxima for $[FeX_4]^{2-}$ with different haloligands illustrate a shift to longer wavelength (lower energy) as the ligand becomes easier to oxidize (I^- easier than Br^-, easier than Cl^-). Finally, a comparison of two osmium complexes that differ only in the oxidation state of the metal centre illustrates that the observed ordering of the λ_{max} values is consistent with Os(IV) being easier to reduce than Os(III).

Metal-to-ligand charge transfer (MLCT) typically occurs when the ligand has a vacant, low-lying π* orbital, for example, CO, py, bpy, phen and other heterocyclic, aromaticligands. Often, the associated absorption occurs in the UV region of the spectrum and is not responsible for producing intensely coloured species. In addition, for ligands where a ligand-centred π*←π transition is possible (e.g. heterocyclic aromatics such as bpy), the MLCT band may be obscured by the π*←π absorption. For $[Fe(bpy)_3]^{2+}$ and $[Ru(bpy)_3]^{2+,}$ the MLCT bands appear in the visible region at 520 and 452 nm, respectively. These are both metal(II) complexes, and the metal d-orbitals are relatively close in energy to the ligand π* orbitals, giving rise to an MLCT absorption energy corresponding to the visible part of the spectrum.

Selection rules

Electronic energy levels are labelled with term symbols. Thus, the term symbol is written in the general form:

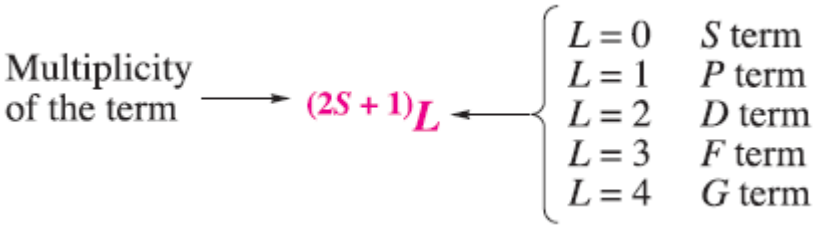

Electronic transitions between energy levels obey the following selection rules.

Spin selection rule: ΔS = 0

Transitions may occur from singlet to singlet, or from triplet to triplet states, and so on. Thus the transition is ***allowed***, but a change in spin multiplicity is ***forbidden*** such as singlet to triplet.

Laporte selection rule: There must be a change in parity:

allowed transitions: g ↔ u

forbidden transitions: g ↔g u↔ u

This leads to the selection rule:

allowed transitions are s → p, p →d , d → f ;

forbidden transitions are s → s, p → p, d → d, f → f ,s → d, p →f etc.

Since these selection rules must be strictly obeyed, why do many d-block metal complexes exhibit ‘d–d’ bands in their electronic spectra?

A spin-forbidden transition becomes ‘allowed’ if, for example, a singlet state mixes to some extent with a triplet state. This is possible by spin–orbit coupling ,but for first row metals, the degree of mixing is small and so bands associated with ‘spin-forbidden’ transitions are very weak (Table pp.73). Spin-allowed ‘d–d’ transitions remain Laporte-forbidden and their observation is explained by a mechanism called ***‘vibronic coupling’***. An octahedral complex possesses a centre of symmetry, but molecular vibrations result in its temporary loss. At an instant when the molecule

does not possess a centre of symmetry, mixing of d and p orbitals can occur. Since the lifetime of the vibration ($\approx 10^{-13}$ s) is longer than that of an electronic transition ($\approx 10^{-18}$ s), a 'd–d' transition involving an orbital of mixed pd character can occur although the absorption is still relatively weak (Table pp 73). In a molecule which is non-centrosymmetric (e.g. tetrahedral), p–d mixing can occur to a greater extent and so the probability of 'd–d' transitions is greater than in a centrosymmetric complex. This leads to tetrahedral complexes being more intensely coloured than octahedral complexes.

Example: Explain why an electronic transition for high-spin $[Mn(OH_2)_6]^{2+}$ is spin-forbidden, but for $[Co(OH_2)_6]^{2+}$ is spin-allowed.

Sol. $[Mn(OH_2)_6]^{2+}$ is high-spin d^5 Mn(II):

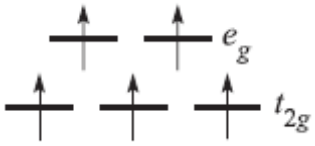

A transition from a t_2g to eg orbital is impossible without breaking the spin selection rule: $\Delta S = 0$, which means that S must remain the same.

$[Co(OH_2)_6]^{2+}$ is a high-spin d^7 Co(II) complex:

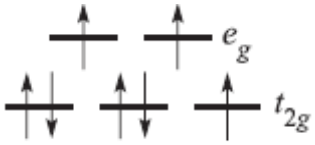

A transition from a t_2g to eg orbital can occur without violating the spin selection rule.

NB: Transitions in both complexes are *Laporte- forbidden.*

Electronic spectra of octahedral and tetrahedral complexes

Electronic spectroscopy is a complicated topic and we shall restrict our discussion to high-spin complexes. This corresponds to the weak field limit. We

begin with the electronic spectrum of an octahedral d^1 ion, exemplified by $[Ti(OH_2)_6]^{3+}$. The spectrum of $[Ti(OH_2)_6]^{3+}$ (Figure pp.71) exhibits one broad band. However, close inspection shows the presence of a shoulder indicating that the absorption is actually two closely spaced bands (see below). The term symbol for the ground state of Ti^{3+} (d^1, one electron with L = 2, S = 1/2) is ^2D. In an octahedral field, this is split into ^2T_2g and ^2Eg terms separated by an energy Δ_{oct}. More generally, it can be shown from group theory that, in an octahedral or tetrahedral field, D, F, G, H and I, but not S and P, terms split. (Lanthanoid metal ions provide examples of ground state H and I terms).

Term	Components in an octahedral field
S	A_{1g}
P	T_{1g}
D	$T_{2g} + E_g$
F	$A_{2g} + T_{2g} + T_{1g}$
G	$A_{1g} + E_g + T_{2g} + T_{1g}$
H	$E_g + T_{1g} + T_{1g} + T_{2g}$
I	$A_{1g} + A_{2g} + E_g + T_{1g} + T_{2g} + T_{2g}$

Similar splittings occur in a tetrahedral field, but the *g* labels are no longer applicable.

The splittings arise because the S, P, D, F, G, H and I terms refer to a degenerate set of d orbitals. In an octahedral field, this splits into the t_2g and eg sets of orbitals (Figure pp.59). For the d^1 ion, there are therefore two possible configurations: $t_2g^1\ eg^0$ or $t_2g^0\ eg^1$, and these give rise to the ^2T_2g (ground state) and ^2Eg (excited state) terms. The energy separation between these states increases with increasing field strength (see Figure below).

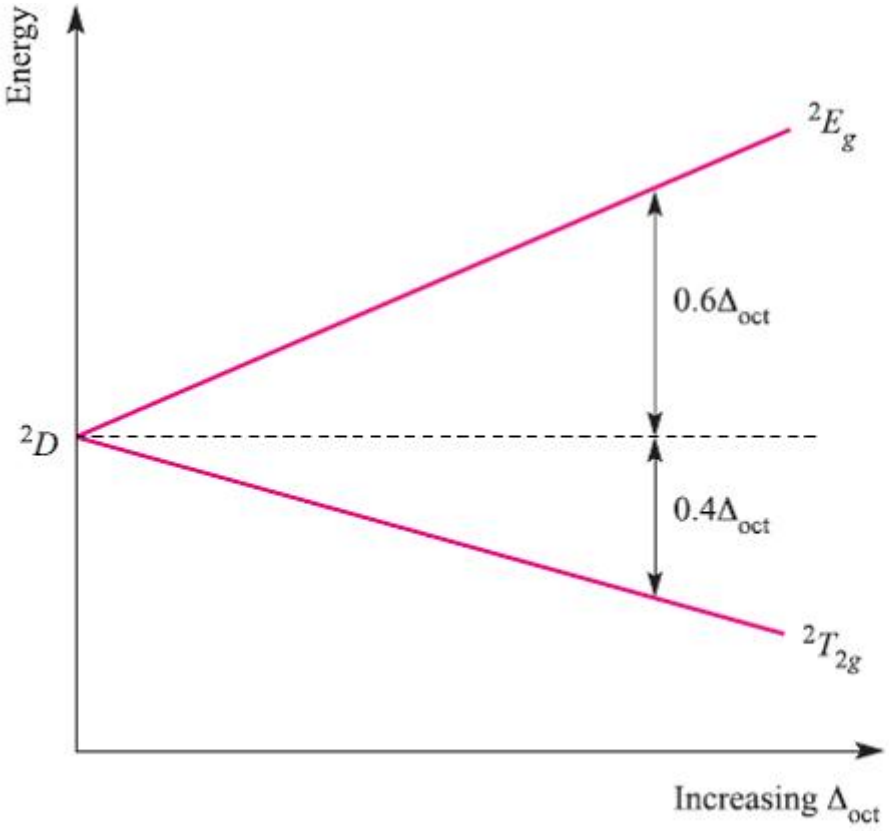

Fig. Energy level diagram for a d^1 ion in an octahedral field.

The electronic spectrum of Ti^{3+} arises from a transition from the T_2g to the Eg level; the energy of the transition depends on the field strength of the ligands in the octahedral Ti(III) complex. The observation that the electronic spectrum of $[Ti(OH_2)_6]^{3+}$ (Figure pp.71) consists of two bands, rather than one, can be rationalized in terms of a Jahn–Teller effect in the excited state, $t_2g^0\ eg^1$.

For the d^9 configuration (e.g. Cu^{2+}) in an octahedral field (actually, a rare occurrence because of Jahn–Teller effects which lower the symmetry), the ground state of the free ion (^2D) is again split into ^2T_2g and ^2Eg terms, but, in contrast to the d^1 ion , the ^2Eg term is lower than the ^2T_2g term. The d^9 and d^1 configurations are related by a positive hole concept: d^9 is derived from a d^{10} configuration by replacing one electron by a positive hole; thus, whereas the d^1 configuration contains one

electron, d^9 contains one 'hole'. For a d^9 ion in an octahedral field, the splitting diagram is an inversion of that for the octahedral d^1 ion. This relationship is shown in Figure below (an **Orgel diagram**) where the right-hand side describes the octahedral d^1 case and the left-hand side describes the octahedral d^9 ion. Just as there is a relationship between the d^1 and d^9 configurations, there is a similar relationship between the d^4 and d^6 configurations. The result is that the Orgel diagrams for octahedral d^1 and d^6 ions are the same, as are the diagrams for octahedral d^4 and d^9 (Figure below).

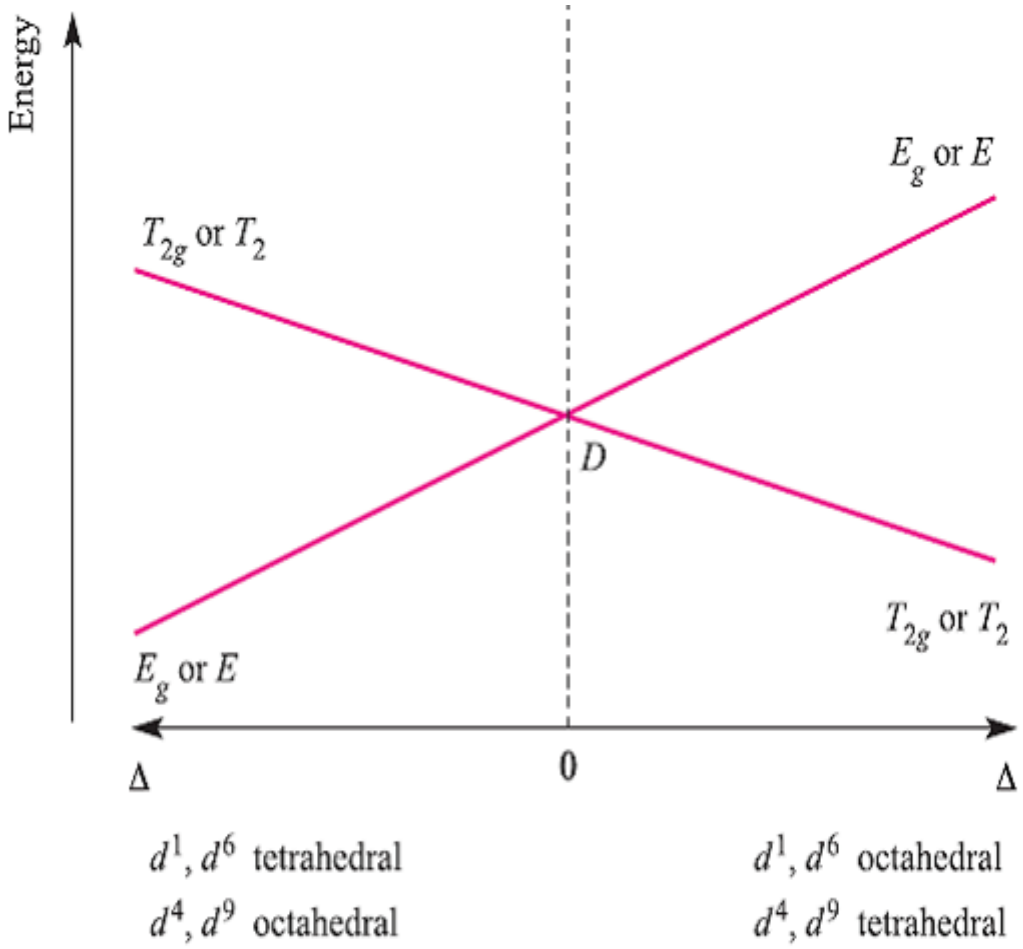

Fig. Orgel diagram for d^1, d^4 (high-spin), d^6 (high-spin) and d^9 ions in octahedral (for which T_{2g} and E_g labels are relevant) and tetrahedral (E and T_2 labels) fields.

Figure above shows that for each of the octahedral and tetrahedral d^1, d^4, d^6 and d^9 ions, only one electronic transition from a ground to excited state is possible:

1) For octahedral d^1 and d^6, the transition is $Eg \leftarrow T_2g$
2) For octahedral d^4 and d^9, the transition is $T_2g \leftarrow Eg$
3) For tetrahedral d^1 and d^6, the transition is $T_2 \leftarrow E$
4) For tetrahedral d^4 and d^9, the transition is $E \leftarrow T_2$

Each transition is spin-allowed (no change in total spin, S) and the electronic spectrum of each ion exhibits one absorption. For sake of completeness, the notation for the transitions given above should include spin multiplicities, 2S+1, e.g. for octahedral d^1, the notation is $^2Eg \leftarrow {}^2T_2g$, and for high-spin, octahedral d^4 it is $^5T_2g \leftarrow {}^5Eg$.

In an analogous manner to grouping d^1, d^4, d^6 and d^9 ions, we can consider together d^2, d^3, d^7 and d^8 ions in octahedral and tetrahedral fields. In order to discuss the electronic spectra of these ions, the terms that arise from the d^2 configuration must be known. In an absorption spectrum, we are concerned with electronic transitions from the ground state to one or more excited states. Transitions are possible from one excited state to another, but their probability is so low that they can be ignored. Two points are particularly important:

1) Selection rules restrict electronic transitions to those between terms with the same multiplicity;
2) The ground state will be a term with the highest spin multiplicity (Hund's rules).

In order to work out the terms for the d^2 configuration, a table of microstates (see Table below) must be constructed. However, for interpreting electronic spectra, we need concern ourselves only with the terms of maximum spin multiplicity. This corresponds to a weak field limit. For the d^2 ion, we therefore focus on the ^3F and ^3P

(triplet) terms. These are summarized in (Table below), with the corresponding microstates represented only in terms of electrons with $m_s = +1/2$.

Table A shorthand table of microstates for a d^2 configuration; only a high-spin case (weak field limit) is considered, and each electron has $m_s = +\frac{1}{2}$. The microstates are grouped so as to show the derivation of the ^3F and ^3P terms.

$m_l = +2$	$m_l = +1$	$m_l = 0$	$m_l = -1$	$m_l = -2$	M_L	
↑	↑				+3	^3F ($L = 3$)
↑		↑			+2	
↑			↑		+1	
↑				↑	0	
	↑			↑	−1	
		↑		↑	−2	
			↑	↑	−3	
	↑	↑			+1	^3P ($L = 1$)
	↑		↑		0	
		↑	↑		−1	

The ^3F term is expected to be lower in energy than the ^3P term. In an octahedral field, the ^3P term does not split, and is labelled ^3T_1g. The ^3F term splits into ^3T_1g, ^3T_2g and ^3A_2g terms. The $^3T_1g(F)$ term corresponds to a $t_2g^2\ eg^0$ arrangement and is triply degenerate because there are three ways of placing two electrons (with parallel spins) in any two of the dxy, dyz and dxz orbitals. The ^3A_2g term corresponds to $t_2g^0\ eg^2$ arrangement (singly degenerate).

The ^3T_2g and $^3T_1g(P)$ terms equate with a $t_2g^1\ eg^1$ configuration; the lower energy ^3T_2g term arises from placing two electrons in orbitals lying in mutually perpendicular planes, e.g.$(dxy)^1\ (dz^2)^1$, while the higher energy $^3T_1g(P)$ term arises from placing two electrons in orbitals lying in the same plane e.g.$(dxy)^1\ (dx^2\text{-}y^2)^1$. The energies of the $^3T_1g(F)$, ^3T_2g, ^3A_2g and $^3T_1g(P)$ terms are shown on the right-hand side of (Figure below); note the effect of increasing field strength. Starting from this diagram and using the same arguments as for the d^1, d^4, d^6 and d^9 ions, we can derive the complete Orgel diagram shown in (Figure below).

From (Figure below), we can see why three absorptions are observed in the electronic spectra of d^2, d^3, d^7 and d^8 octahedral and tetrahedral complexes. The transitions are from the ground to excited states, and are all spin-allowed, e.g. for an octahedral d^3 ion, the allowed transitions are $^4T_2g \leftarrow {}^4A_2g$, $^4T_1g(F) \leftarrow {}^4A_2g$ and $^4T_1g(P) \leftarrow {}^4A_2g$.

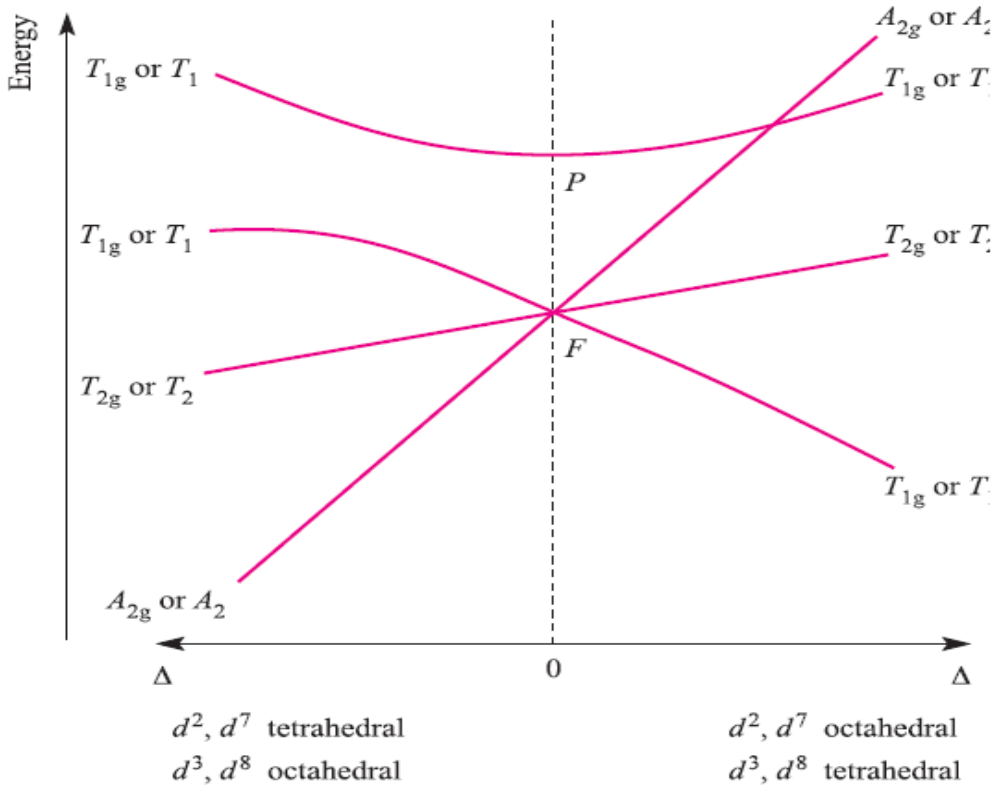

Fig. Orgel diagram for d^2, d^3, d^7 and d^8 ions (high-spin) in octahedral (for which T_{1g}, T_{2g} and A_{2g} labels are relevant) and tetrahedral (T_1, T_2 and A_2 labels) fields. Multiplicities are not stated because they depend on the d^n configuration, e.g. for the octahedral d^2 ion, $^3T_{1g}$, $^3T_{2g}$ and $^3A_{2g}$ labels are appropriate.

Figure below illustrates spectra for octahedral nickel(II) (d^8) complexes. For the high-spin d^5 configuration, all transitions are spin forbidden and 'd–d' transitions that are

observed are between the ^6S ground state and quartet states (three unpaired electrons). Associated absorptions are extremely weak.

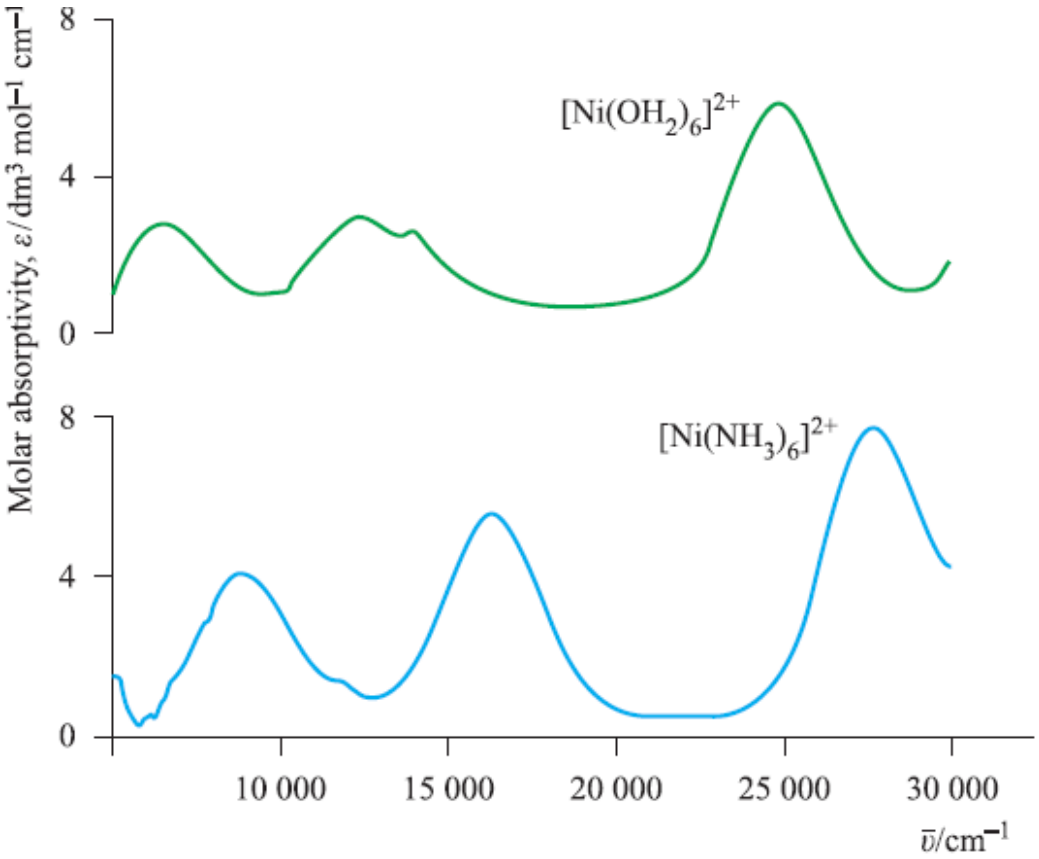

Fig. Electronic spectra of $[Ni(OH_2)_6]^{2+}$ (0.101 mol dm^{-3}) and $[Ni(NH_3)_6]^{2+}$ (0.315 mol dm^{-3} in aqueous NH_3 solution) showing three absorption bands. Values of the molar absorptivity, ε, are related to absorbance by the Beer–Lambert law